Edaravone (MCI-186, 3-methyl-1-phenyl-2-pyrazolin-5-one, Mitsubishi Tanabe Pharma Corporation, Tokyo, Japan) is a free radical scavenger approved for treatment of acute cerebral infarction in Japan in 2001 (13). Edaravone eliminates lipid peroxides and hydroxyl radicals during cerebral ischemia and protects nerve cells within or around the ischemic region from free radical damage (14–16). Beneficial effects of edaravone have been reported in wobbler mice with ALS-like symptoms (17) and in ALS-model animals (18,19).

A phase II trial was conducted to investigate the safety and efficacy of edaravone in ALS patients, and found that progression of motor dysfunction was slowed and no clinically significant adverse drug reactions occurred. The level of 3NT was low in cerebrospinal fluid of almost all patients in the phase II trial, suggesting that edaravone could protect neuronal cells from oxidative stress (20). Therefore we designed a clinical trial to confirm the efficacy and safety of edaravone in ALS patients.

Methods

Standard protocol approvals

Twenty-nine sites in Japan participated in the study between May 2006 and September 2008. An institutional review board at each site approved the study protocol. The study was conducted in compliance with Good Clinical Practice (GCP). All participants provided written informed consent before the pre-observation stage. The study sponsor was Mitsubishi Tanabe Pharma Corporation. The study is registered in ClinicalTrials.gov with a registration number NCT00330681.

Patients

Inclusion criteria were: age 20–75 years; diagnosis of 'definite', 'probable' or 'probable laboratory-supported' ALS (21,22) according to the revised Airlie House diagnostic criteria; forced vital capacity (FVC) of at least 70%; duration of disease within three years; and change in revised ALS functional rating scale (ALSFRS-R) (23,24) score during the 12-week pre-observation period of –1 to –4 points. Patients also had a Japanese ALS severity classification (25) of 1 or 2. (The Japanese ALS severity classification score ranges from 1 to 5 according to the severity classification of the Specified Disease Treatment Research Program for ALS of the Ministry of Health, Labor and Welfare of Japan. Severity Classification: 1) able to work or perform housework; 2) independent living but unable to work; 3) requiring assistance for eating, excretion or ambulation; 4) presence of respiratory insufficiency, difficulty in coughing out sputum or dysphagia; and 5) using a tracheostomy tube, tube feeding or tracheostomy positive pressure ventilation.)

Exclusion criteria were: reduced respiratory function and complaints of dyspnea; complications that may substantially influence evaluation of drug efficacy, such as Parkinson's disease, schizophrenia and dementia; complications that require hospitalization, including liver, cardiac and renal diseases; infections that require antibiotic therapy; deteriorated general condition as judged by investigators; renal dysfunction with creatinine clearance of 50 ml/min or below within 28 days before treatment; and undergoing cancer treatment.

Patient eligibility was assessed with inclusion and exclusion criteria at the start and end of pre-observation.

Administration regimen of riluzole was required not to be changed during the study.

Study medication

Mitsubishi Tanabe Pharma Corporation provided the investigational drugs in ampoules. Only authorized personnel, independent of the sponsor and investigators, had access to the key code until unblinding. The dose of edaravone was 60 mg per day, which was indicated to show efficacy in the phase II trial (20), and placebo was chosen since no suitable comparator drug for ALS has been approved. Saline (placebo) or edaravone was administered once daily by i.v. infusion over 60 min.

Design

After the 12-week pre-observation period, eligible patients were randomized to placebo or edaravone group. Dynamic allocation was used to minimize the effects of the following three factors, which may substantially influence the evaluation of edaravone:

- Factor 1: change in ALSFRS-R score during pre-observation period: two categories: –4, –3 or –2, –1.
- Factor 2: initial symptom: two categories – bulbar or limb.
- Factor 3: use of riluzole: two categories – yes or no.

The study period was 36 weeks, consisting of a 12-week pre-observation period before the start of the first cycle, followed by a 24-week treatment period (Figure 1).

A single treatment cycle consisted of 14 days of study drug administration period followed by a 14-day observation period. Study drugs were administered every day for 14 days in the administration period of the first cycle, and for 10 out of 14 days in the administration periods of cycles 2 to 6. The end of the administration period in each cycle was followed by a 14-day observation period.

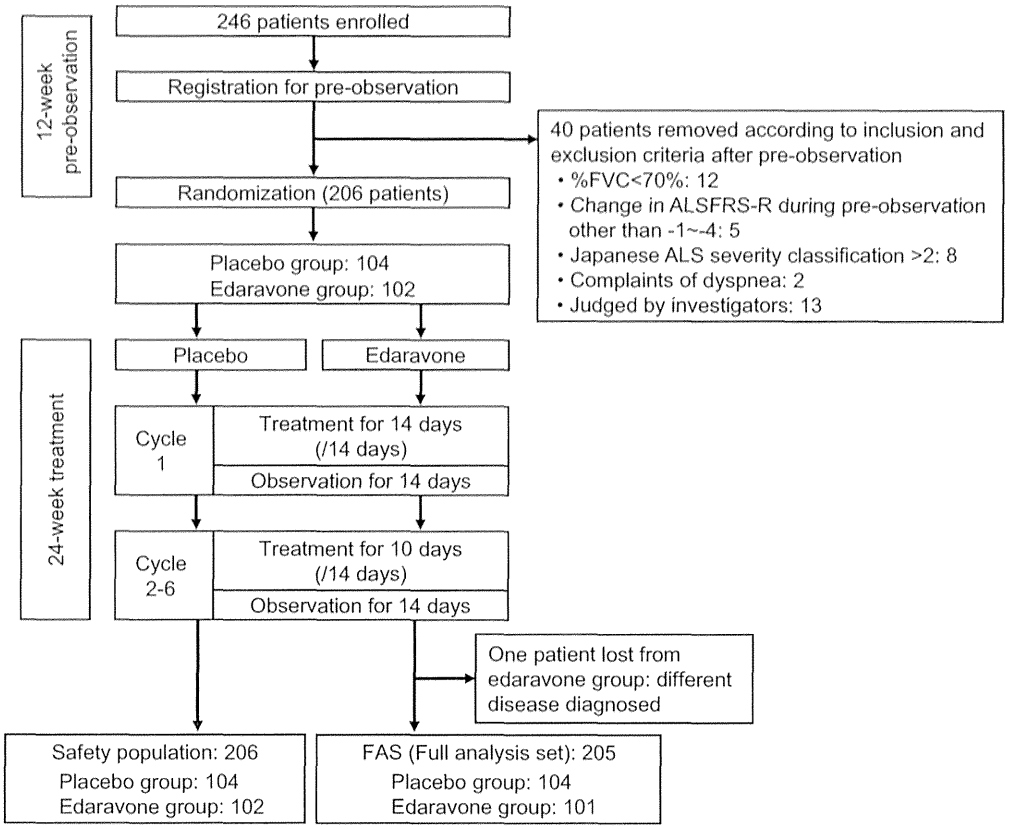

Figure 1. Trial profile.

Efficacy evaluation

Primary efficacy endpoint was the change in ALSFRS-R score. Secondary endpoints were: changes of FVC, grip strength (left/right mean), pinch strength (left/right mean), Modified Norris Scale score (26,27), ALSAQ-40 (ALS Assessment Questionnaire) (28,29), and time to death or a specified state of disease progression (incapable of independent ambulation, loss of function in upper limbs, tracheotomy, artificial respirator with intubation, or tube feeding). The evaluations were carried out at the following times: before pre-observation, before the start of the first treatment cycle and at the end of each treatment cycle (after 14 days observation and before the first dosage of the next cycle).

Safety evaluation

Safety was assessed in terms of number and severity of adverse events (AE), adverse drug reactions and the results of clinical laboratory tests and sensory tests. Serious adverse events were identified from the adverse events according to the GCP guideline.

Statistical analysis

Based upon the experience of the phase II trial (20), we considered that it would be difficult to enroll more than 100 patients per group for the trial and the target number of patients for enrollment was set at 200. In the phase II trial, the difference of the change of ALSFRS-R between the edaravone and placebo groups was 2.2 for patients with matched severity and dose to those of the present study; and on the assumption of a standard deviation of 5.2, the statistical power of this study can be calculated as 85% when 100 patients per group were enrolled.

The primary population used for the efficacy analysis was the full analysis set (FAS). For ALSFRS-R scores, analysis of covariance (ANCOVA) was performed on the change in score during treatment, defined as the difference between the score before the start of the first treatment cycle (before treatment) and the score at two weeks after the end of the sixth treatment cycle (after treatment). Three factors were used for dynamic allocation as covariates, after which the inter-group difference was assessed. Repeated measures analysis of variance was also performed using the treatment group, period, and interaction between treatment group and period (treatment group × period) as design factors, and baseline value and the three factors used for dynamic allocation as covariates, after which the inter-group difference was assessed. Compound symmetry was assumed as a covariance structure of repeated measurement. Edaravone efficacy would be verified if a significant inter-group difference were found in at least one of the above analyses. A two-sided level of significance of 5% and a two-sided 95% confidence interval were chosen for interpretation of main effect. A two-sided level of significance of 15% was chosen for

determining the existence of effect of interaction. A stratified analysis was also performed on the changes of ALSFRS-R score by diagnostic category. The level of significance for differences of patient characteristics was set at 15%.

ANCOVA and repeated measures analysis of variance were similarly performed on the secondary endpoints. Time to death or a specified state of disease progression was defined as an event and the other endpoints were followed until cut-off. A stratified, generalized Wilcoxon test and log-rank test were performed using the change in ALSFRS-R score during the pre-observation period as a stratification factor. For patients with more than one event, the onset date of the first event was defined as the survival time. In censored cases, the cut-off date was the end date of observations.

For patients with missing data at 24 weeks after starting treatment, the last observation carried forward (LOCF) method was applied to impute missing data. Patients who completed the third cycle were eligible for LOCF.

To evaluate safety, AE and adverse drug reactions were assessed in the safety population. Proportions of AE, adverse drug reactions, serious adverse events (SAE) and serious adverse drug reactions were calculated and compared between the groups using Fisher's exact test. A two-sided level of significance of 5% and a two-sided 95% confidence interval were chosen for interpretation. Statistical analysis was performed using SAS software (version 9.1, SAS Institute, Cary, NC).

Results

Subject background

Two hundred and forty-six patients were prospectively registered. After the 12-week pre-observation period, 40 patients were excluded according to the inclusion and exclusion criteria, and the remaining 206 patients were randomized (Figure 1).

The FAS included 205 patients after exclusion of one patient who was diagnosed with a different disease. For the safety evaluation, the number of patients in the safety population was 206, which included all patients treated with the study medication. The treatment was discontinued for 23 patients (edaravone group: patients' request 5, AE 3, tracheotomy 1; placebo group: patients' request 5, AE 6, tracheotomy 2, protocol violation 1). There was no imbalance between the groups in either analysis set on discontinuation (FAS: $p = 0.378$; safety population: $p = 0.377$).

All patients in the safety population received at least 80% of the assigned dosages of study drug.

Patient characteristics are summarized in Table I. Among the patient characteristics, those for which inter-group differences were found at a significance level below 15% were the duration of disease ($p = 0.104$, paired t-test), ALSFRS-R score before pre-observation ($p = 0.065$, paired t-test), and ALSFRS-R score at the start of the first cycle ($p = 0.146$, paired t-test).

Table I. Subject demographic characteristics.

Item	Placebo (104) *n* (%)	Edaravone (101) *n* (%)
Gender		
male	69 (66.3)	63 (62.4)
Initial symptom		
bulbar	20 (19.2)	18 (17.8)
limb	84 (80.8)	83 (82.2)
Diagnosis (El Escorial revisited)		
definite	21 (20.2)	29 (28.7)
probable	54 (51.9)	52 (51.5)
probable laboratory-supported	28 (26.9)	20 (19.8)
possible	1 (1.0)	0 (0.0)
The Japanese severity classification		
grade 1	40 (38.5)	36 (35.6)
grade 2	64 (61.5)	65 (64.4)
Use of riluzole		
yes	92 (88.5)	90 (89.1)
Change in ALSFRS-R score during pre-observation		
−4, −3	32 (30.8)	29 (28.7)
−2, −1	72 (69.2)	72 (71.3)
Item	**Placebo (104) median (min-max)**	**Edaravone (101) median (min-max)**
Age (years old)	58.5 (28–75)	58.0 (29–73)
Body weight (kg)	57.0 (37–109)	57.0 (35–77)
Duration of disease (years)	1.20 (0.3–3.0)	1.30 (0.4–2.9)
ALSFRS-R score before pre-observation	44.0 (35–48)	43.0 (31–48)
ALSFRS-R score before treatment period	42.0 (32–47)	41.0 (29–47)

ALSFRS-R: the revised amyotrophic lateral sclerosis functional rating scale.

Table II. Change in endpoints during treatment.

	Change in endpoints during treatment (ANCOVA)				Repeated-measures analysis			
	Adjusted mean change LS Mean ± S.E.		Inter-group difference in adjusted mean change LS Mean ± S.E. (95% C.I.)	p value	Adjusted mean LS Mean ± S.E.		Inter-group difference in adjusted mean LS Mean ± S.E. (95% C.I.)	p value
	Placebo	Edaravone			Placebo	Edaravone		
Primary endpoint								
ALSFRS-R	−6.35 ± 0.84 (99)	−5.70 ± 0.85 (100)	0.65 ± 0.78 (−0.90 – 2.19)	0.411	37.43 ± 0.46	38.08 ± 0.47	0.65 ± 0.44 (−0.22 – 1.52)	0.141
Secondary endpoint								
%FVC	−17.49 ± 2.39 (99)	−14.57 ± 2.41 (100)	2.92 ± 2.24 (−1.49, 7.33)	0.193	87.30 ± 1.56	88.56 ± 1.59	1.26 ± 1.46 (−1.63, 4.15)	0.390
Grip strength	−5.71 ± 0.69 (99)	−4.81 ± 0.69 (100)	0.89 ± 0.64 (−0.37, 2.16)	0.165	13.22 ± 0.42	13.83 ± 0.43	0.60 ± 0.40 (−0.18, 1.38)	0.130
Pinch strength	−1.03 ± 0.15 (99)	−0.83 ± 0.15 (100)	0.20 ± 0.14 −0.08, 0.48)	0.165	2.62 ± 0.11	2.83 ± 0.11	0.21 ± 0.10 (0.01, 0.41)	0.038
Modified Norris scale	−16.15 ± 2.00 (97)	−14.12 ± 2.05 (95)	2.03 ± 1.89 (−1.69, 5.75)	0.284	NA	NA	NA	NA
ALSAQ40	19.13 ± 3.79 (95)	19.60 ± 3.82 (95)	0.48 ± 3.50 (−6.44, 7.39)	0.892	NA	NA	NA	NA

ALSFRS-R: interaction between treatment group and period ($p = 0.915$). ALSFRS-R: the revised amyotrophic lateral sclerosis functional rating scale. NA: not applicable. For Modified Norris scale and ALSAQ40, repeated measures analysis was not conducted

Efficacy

The results of ANCOVA for the change of ALSFRS-R score during treatment and the results of repeated measures analysis of variance are shown in Table II. In both analyses, no significant inter-group difference was observed.

The changes in ALSFRS-R score during treatment according to diagnostic category, i.e. 'definite', 'probable' and 'probable laboratory-supported', are shown in Figure 2.

The results of secondary endpoints are presented in Table II. The pinch strength analyzed by repeated measures analysis of variance showed a statistically significant difference, as there was no interaction between the treatment group and period ($p = 0.292$). The other endpoints did not show a significant difference.

The proportion of events of death or a particular state of disease progression was documented in 27 patients in the placebo group (14 patients with –4, –3 change in ALSFRS-R score during pre-observation, and 13 patients with –2, –1 change) and 32 in the edaravone group (12 patients with –4, –3 change and 20 patients with –2, –1 change). There was no significant inter-group difference (stratified log-rank test: $p = 0.381$, stratified generalized Wilcoxon test: $p = 0.399$).

Safety

The proportion of AE reported in the safety population was 88.5% in the placebo group and 89.2% in the edaravone group. All AE and SAE with a proportion of at least 5% in either group are listed (Table III). The inter-group difference in proportion with 95% confidence interval is 0.8% (–7.8% to 9.4%). There were no significant inter-group differences in the proportion of AE ($p = 1.000$), and in adverse drug reactions ($p = 0.349$). The proportion of SAE was 23.1% in the placebo group and 17.6% in the edaravone group. Two cases of respiratory failure in the placebo group resulted in death; in the edaravone group, there were three deaths (two cases of respira-

Figure 2. Change of ALSFRS-R score during treatment by diagnostic category. ALSFRS-R: the revised amyotrophic lateral sclerosis functional rating scale.

Table III. Adverse events and serious adverse events.

	AE				SAE			
	Placebo (104)		Edaravone (102)		Placebo (104)		Edaravone (102)	
Treatment	*n*	(%)	*n*	(%)	*n*	(%)	*n*	(%)
Total	92	(88.5)	91	(89.2)	24	(23.1)	18	(17.6)
Constipation	17	(16.3)	13	(12.7)				
Dysphagia	12	(11.5)	8	(7.8)	11	(10.6)	8	(7.8)
Nasopharyngitis	22	(21.2)	22	(21.6)				
Muscular weakness	9	(8.7)	7	(6.9)	1	(1.0)	1	(1.0)
Contusion	5	(4.8)	12	(11.8)				
Headache	3	(2.9)	8	(7.8)				
Insomnia	10	(9.6)	9	(8.8)				
Gait disturbance	16	(15.4)	20	(19.6)	2	(1.9)	3	(2.9)
Eczema	2	(1.9)	7	(6.9)				
Glucose urine present	3	(2.9)	6	(5.9)				

All AE with an incidence greater than 5% are tabulated by the primary term, MedDRA version 11.1.

tory disorder and one case of respiratory failure). The investigators determined that the deaths were due to the primary disease and were not related to the study drug. There was no significant inter-group difference in the proportion of SAE ($p = 0.389$). No serious adverse drug reactions occurred in either group.

Discussion

The results of prior clinical trials (20,30) indicated that edaravone may delay the progression of symptoms in some ALS patients. Because evaluation of edaravone would be difficult in patients in whom ALS progression was either acute or non-existent, only patients whose ALSFRS-R score changed by –1 to –4 points during the 12-week pre-observation period were eligible for the study. Since efficacy was found over the 24-week treatment period in the phase II trial, a treatment period of 24 weeks was also chosen for this study.

Based on the results of the previous phase II trial, the inter-group difference in the change of ALSFRS-R score at the end of treatment was expected to be 2 points in this trial. However, the actual inter-group difference was only 0.65 points by ANCOVA and this was not statistically significant. No significant inter-group difference was found by repeated measures analysis of variance either. The results of ANCOVA for pinch strength, a secondary endpoint, suggested a beneficial effect in the edaravone group compared to the placebo group.

Additionally, stratified analysis by diagnostic category (Figure 2) revealed that the change in ALSFRS-R score during treatment was greater in those patients fulfilling the criteria for clinically definite ALS using the Airlie House diagnostic classification. This trial enrolled patients with longer duration of disease and higher ALSFRS-R scores at the start of treatment compared to those of the patients in other trials (31–34). As shown in Table I, the mean duration of disease for the edaravone group and the placebo group was 1.3 years and 1.2 years, respectively, and the mean ALSFRS-R score at the start of treatment was 41 and 42, respectively. While the mean change in ALSFRS-R score during the treatment was –5.70 for the edaravone group and –6.35 for the placebo group, our internal analysis showed that 25% of patients in the edaravone group and 26% of patients in the placebo group showed the change of 0 or –1 point in ALSFRS-R score indicating a more slowly progressive form of the disease than had originally been anticipated when the trial was designed, and thus attenuating the power of the study. Future trials will aim to enroll patients with more rapidly progressive illness. AE occurred in nearly 90% of both groups, i.e. 88.5% of patients in the placebo group and 89.2% in the edaravone group, with no significant differences between the two groups.

In conclusion, although the elimination of free radicals to inhibit the degeneration of motor neurons appears to be a promising new strategy for the treatment of ALS, this study failed to demonstrate efficacy of edaravone to delay the progression of ALS. While the primary endpoint was not achieved, we consider that the results are helpful to identify the patient population in which edaravone could be expected to show efficacy. On the basis of this information, we have designed and are conducting a phase III study.

Acknowledgements

The authors thank all participating patients and their family members, and all the investigators and study coordinators at the 29 centers involved in the trial. Thanks are also due to Mitsubishi Tanabe Pharma Corporation for monitoring of the study, data collection and management, and statistical analysis.

The Edaravone ALS Study Group: Site Investigators

MCI-186 ALS study group investigators are as follows.

Hokkaido University Hospital, Sapporo: Hidenao Sasaki; Hokuyukai Neurological Hospital, Sapporo: Asako Takei, Isao Yamashita; Tohoku University Hospital, Sendai: Masashi Aoki; National Hospital Organization Miyagi National Hospital, Watari: Takashi Imai; Jichi Medical School Hospital, Shimotsuke: Imaharu Nakano; Gunma University Hospital, Maebashi: Koichi Okamoto; Saitama Center of Neurology and Psychiatry, Saitama: Yuichi Maruki; Kohnodai Hospital, National Center for Global Health and Medicine, Ichikawa: Shuichi Mishima, Jin Nishimiya; Toho University Omori Medical Center, Tokyo: Yasuo Iwasaki; Nippon Medical School Hospital, Tokyo: Mineo Yamazaki; The University of Tokyo Hospital, Tokyo: Yuji Takahashi; Kitasato University East Hospital, Sagamihara: Mieko Ogino, Yutaka Ogino; National Center of Neurology and Psychiatry, Kodaira: Masafumi Ogawa; Shonan Fujisawa Tokushukai Hospital, Chigasaki: Tetsumasa Kamei; Seirei Hamamatsu General Hospital, Hamamatsu: Tsuyoshi Uchiyama; Nagoya University Hospital, Nagoya: Hirohisa Watanabe; Mie University Hospital, Tsu: Yasumasa Kokubo; National Hospital Organization Utano Hospital, Kyoto: Hideyuki Sawada; Osaka General Medical Center, Osaka: Takanori Hazama; Osaka Medical College Hospital, Takatsuki: Fumiharu Kimura; National Hospital Organization Toneyama National Hospital, Toyonaka: Harutoshi Fujimura; Kansai Medical University Takii Hospital, Moriguchi: Hirofumi Kusaka; Okayama University Hospital, Okayama: Koji Abe; National Hospital Organization Ehime National Hospital, Toon: Tsukasa Hashimoto; Saiseikai Fukuoka General Hospital, Fukuoka: Takeshi Yamada, Kanamori Yuji, Yamasaki Kenji; Fukuoka Tokushukai Medical Center, Kasuga: Shizuma Kaku; Murakami Karindou Hospital, Fukuoka: Hitoshi Kikuchi; National Hospital Organization Kumamoto Saishunso National Hospital, Koshi: Shigehiro Imamura; National Hospital Organization Miyazaki Higashi Hospital, Miyazaki: Seiichiro Sugimoto, Kishi Masahiko.

Declaration of interest: K. Abe received funding for travel and speaker honoraria from Mitsubishi Tanabe Pharma Corp. Y. Itoyama received speaker honoraria from Mitsubishi Tanabe Pharma Corp. G. Sobue received funding for travel and speaker honoraria from Mitsubishi Tanabe Pharma Corp, and serves on the scientific advisory board for the Kanae Science Foundation for the Promotion of Medical Science, Naito Science Foundation and serves as an advisory board member of Brain, an editorial board member of Degenerative Neurological and Neuromuscular Disease, the Journal of Neurology, and Amyotrophic Lateral Sclerosis and Frontotemporal Degeneration, and received funding from the Ministry of Education, Culture, Sports, Science and Technology of Japan; the Ministry of Welfare, Health and Labor of Japan; the Japan Science and Technology Agency, Core Research for Evolutional Science and Technology. S. Tsuji received funding for travel and speaker honoraria from Mitsubishi Tanabe Pharma Corp. M. Aoki received speaker honoraria, travel expenses, and fees for conducting and consulting on pharmacological test of edaravone in a rat ALS model, from Mitsubishi Tanabe Pharma Corp, and has received research grants, Research on Nervous and Mental Disorders, Research on Measures for Intractable Diseases, Research on Psychiatric and Neurological Diseases and Mental Health from the Japanese Ministry of Health Labor and Welfare, Grants-in-Aid for Scientific Research, an Intramural Research Grant for Neurological Psychiatric Disorders from NCNP and Grants-in-Aid for Scientific Research from the Japanese Ministry of Education, Culture, Sports, Science and Technology. M. Doyu received funding for travel or speaker honoraria from Mitsubishi Tanabe Pharma Corp. C. Hamada is a consultant for Chugai Pharmaceutical Co. Ltd., Taiho Pharmaceutical Co. Ltd., Kowa Company Ltd., Sanwa Kagaku Kenkyusho Co. Ltd., Maruho Co. Ltd., Daiichi Sankyo Co. Ltd., Eisai Co. Ltd., Mochida Pharmaceutical Co. Ltd., Otsuka Pharmaceutical Co. Ltd., Nippon Shinyaku Pharmaceutical Co. Ltd. and Mitsubishi Tanabe Pharma Corp. K. Kondo is an employee of Mitsubishi Tanabe Pharma Corporation. T. Yoneoka is an employee of and co-owns a patent with Mitsubishi Tanabe Pharma Corporation. M. Akimoto is an employee of Mitsubishi Tanabe Pharma Corporation. Y. Yoshino received funding for speaker honoraria from, co-owns a patent with, and is a consultant for Mitsubishi Tanabe Pharma Corp.

The study was funded by Mitsubishi Tanabe Pharma Corporation.

The authors alone are responsible for the content and writing of the paper.

References

1. Rowland LP, Shneider NA. Amyotrophic lateral sclerosis. N Engl J Med. 2001;344:1688–700.
2. Chio A, Logroscino G, Hardiman O, Swingler R, Mitchell D, Beghi E, et al. Prognostic factors in ALS: a critical review. Amyotroph Lateral Scler. 2009;10:310–23.
3. Beckman JS, Carson M, Smith CD, Koppenol W. ALS, SOD and peroxynitrite. Nature. 1993;364:584.
4. Ferrante RJ, Shinobu LA, Schulz JB, Matthews RT, Thomas CE, Kowall NW, et al. Increased 3-nitrotyrosine and oxidative damage in mice with a human Cu/Zn superoxide disumutase mutation. Ann Neurol. 1997;42:326–34.
5. Beal MF, Ferrante RJ, Browne SE, Matthews RT, Kowall NW, Brown RH Jr. Increased 3-nitrotyrosine in both sporadic and familial amyotrophic lateral sclerosis. Ann Neurol. 1997;42:644–54.
6. Abe K, Pan LH, Watanabe M, Kato T, Itoyama Y. Induction of nitrotyrosine-like immunoreactivity in the lower motor

neuron of amyotrophic lateral sclerosis. Neurosci Lett. 1995;199:152–4.
7. Sasaki S, Shibata N, Komori T, Iwara M. iNOS and nitrotyrosine immunoreactivity in amyotrophic lateral sclerosis. Neurosci Lett. 2000;291: 44–8.
8. Tohgi H, Abe T, Yamazaki K, Murata T, Ishizaki E, Isobe C. Remarkable increase in cerebrospinal fluid 3-nitotyrosine in patients with sporadic amyotrophic lateral sclerosis. Ann Neurol. 1999;46:129–31.
9. Itoh K, Wakabayashi N, Katoh Y, Ishii T, Igarashi K, Engel JM, et al. Keap1 represses nuclear activation of antioxidant responsive elements by Nrf2 through binding to the amino-terminal Neh2 domain. Genes Dev. 1999;13:76–86.
10. Arai T, Hasegawa M, Akiyama H, Ikeda K, Nonaka T, Mori H, et al. TDP-43 is a component of ubiquitin-posive tau-negative inclusions in frontotemporal lobar degeneration and amyotrophic lateral sclerosis. Biochem Biophys Res Commun. 2006:351;602–11.
11. Neumann M, Sampathu DM, Kwong LK, Truax AC, Micsenyi MC, Chou TT, et al. Ubiqutinated TDP-43 in frontotemporal lobar degeneration and amyotrophic lateral sclerosis. Science. 2006:314;130–3.
12. Duan W, Li X, Shi J, Guo Y, Li Z, Li C. Mutant TAR DNA-binding protein-43 induces oxidative injury in motor neuron-like cell. Neuroscience. 2010:169;1621–9.
13. The Edaravone Acute Brain Infarction Study Group. Effect of a novel free radical scavenger, edaravone (MCI-186), on acute brain infarction. Cerebravascuar Dis. 2003;15:222–9.
14. Watanabe T, Yuki S, Egawa M, Nishi H. Protective effects of MCI-186 on cerebral ischemia: possible involvement of free radical scavenging and antioxidant actions. J Pharmacol Exp Ther. 1994;268:1597–1604.
15. Mizuno A, Umemura K, Nakashima M. Inhibitory Effect of MCI-186, a free radical scavenger, on cerebral ischemia following the rat middle cerebral artery occlusion. Gen Pharmacol. 1998;30:575–8.
16. Yamamoto T, Yuki S, Watanabe T, Mitsuka M, Saito K, Kogure K. Delayed neuronal death prevented by inhibition of increased hydroxyl radical formation in a transient cerebral ischemia. Brain Research. 1997;762:240–2.
17. Ikeda K, Iwasaki Y, Kinoshita M. Treatment of wobbler mice with free radical scavenger. Molecular Mechanism and Therapeutics of Amyotrophic Lateral Sclerosis. Elsevier Science B.V. 2001;335–40.
18. Ito H, Wate R, Zhang J, Ohnishi S, Kaneko S, Ito H, et al. Treatment with edaravone, initiated at symptom onset, slows motor decline and decreases SOD1 deposition in ALS mice. Exp Neurol. 2008;213:448–55.
19. Aoki M, Warita H, Mizuno H, Suzuki N, Yuki S, Itoyama Y. Feasibility study for functional test battery of SOD transgenic rat (H46R) and evaluation of edaravone, a free radical scavenger. Brain Res. 2011;25:321–5.
20. Yoshino H, Kimura A. Investigation of the therapeutic effects of edaravone, a free radical scavenger, on amyotrophic lateral sclerosis (phase II study). Amyotroph Lateral Scler. 2006; 7:241–5.
21. Brooks BR. Introduction defining optimal management in ALS: from first symptoms to announcement. Neurology. 1999;53:S1–3.
22. Brooks BR, Miller RG, Swash M, Munsat TL. El Escorial revisited: revised criteria for the diagnosis of amyotrophic lateral sclerosis. Amyotroph Lateral Scler Other Motor Neuron Disord. 2000;1:293–9.
23. Cedarbaum JM, Stambler N, Malta E, Fuller C, Hilt D, Thurmond B, et al. The ALSFRS-R: a revised ALS functional rating scale that incorporates assessments of respiratory function. J Neurol Sci. 1999;169:13–21.
24. Ohashi Y, Tashiro K, Itoyama Y, Nakano I, Sobue G, Nakamura S, et al. Study of functional rating scale for amyotrophic lateral sclerosis: revised ALSFRS (ALSFRS-R) Japanese Version. No To Shinkei. 2001;53:346–55. (In Japanese.)
25. Japan intractable diseases information center[online]. Available at: http://www.nanbyou.or.jp/entry/52. Accessed November 13, 2012.
26. Lacomblez L, Bouche P, Bensimon G, Meininger V. A double-blind, placebo-controlled trial of high doses of gangliosides in amyotrophic lateral sclerosis. Neurology. 1989;39:1635–7.
27. Oda E, Ohashi Y, Tashiro K, Mizuno Y, Kowa H, Yanagisawa N. Reliability and factorial structure of a rating scale for amyotrophic lateral sclerosis. No To Shinkei. 1996;48:999–1007. (In Japanese.)
28. Jenkinson C, Fitzpatrick R, Brennen C, Swash M. Evidence for the validity and reliability of the ALS assessment questionnaire: the ALSAQ-40. Amyotroph Lateral Scler Other Motor Neuron Disord. 1999;1:33–40.
29. Yamaguchi T, Ohbu S, Ito Y, Moriwaka F, Tashiro K, Ohashi Y, et al. Validity and clinical applicability of the Japanese version of amyotrophic lateral sclerosis: Assessment questionnaire 40(ALSAQ-40). No To Shinkei. 2004;56: 483–94. (In Japanese.)
30. Yoshino H, Kimura A. Clinical trial for amyotrophic lateral sclerosis with free radical scavenger, edaravone. Neurol Therap. 2003;20:557–64. (In Japanese.)
31. Dupuis L, Dengler R, Heneka MT, Meyer T, Zierz S, Kassubek J, et al. A randomized, double-blind, placebo-controlled trial of pioglitazone in combination with riluzole in amyotrophic lateral sclerosis. PlosOne. 2012;7;6; e37885.
32. Cudkowicz M, Bozik ME, Ingersoll EW, Miller R, Mitsumoto H, Shefner J, et al. The effects of dexpramipexole (KNS-76704) in individuals with amyotrophic lateral sclerosis. Nat Med. 2011;17:1652–6.
33. Pascuzzi RM, Shefner J, Chappell AS, Bjerke JS, Tamura R, Chaudhry V, et al. A phase II trial of talampanel in subjects with amyotrophic lateral sclerosis. Amyotroph Lateral Scler. 2010;11:266–71.
34. Meininger V, Drory VE, Leigh PN, Ludolph A, Robberecht W, Silani V. Glatiramer acetate has no impact on disease progression in ALS at 40 mg/day: a double-blind, randomized, multicentre, placebo-controlled trial. Amyotroph Lateral Scler. 2009;10:378–83.

Human Molecular Genetics, 2015, Vol. 24, No. 2 **314–329**
doi:10.1093/hmg/ddu445
Advance Access published on August 28, 2014

Pioglitazone suppresses neuronal and muscular degeneration caused by polyglutamine-expanded androgen receptors

Madoka Iida[1], Masahisa Katsuno[1,*], Hideaki Nakatsuji[1], Hiroaki Adachi[1], Naohide Kondo[1], Yu Miyazaki[1], Genki Tohnai[1], Kensuke Ikenaka[1], Hirohisa Watanabe[1], Masahiko Yamamoto[2], Ken Kishida[3,4] and Gen Sobue[1,*]

[1]Department of Neurology, Nagoya University Graduate School of Medicine, Nagoya, Aichi 466-8550, Japan, [2]Department of Speech Pathology and Audiology, Aichi-Gakuin University School of Health Science, Nisshin, Aichi 470-0195, Japan, [3]Department of Metabolic Medicine, Graduate School of Medicine, Osaka University, Suita, Osaka 565-0871, Japan and [4]Kishida Clinic, Toyonaka, Osaka 560-0021, Japan

Received May 13, 2014; Revised July 30, 2014; Accepted August 26, 2014

Spinal and bulbar muscular atrophy (SBMA) is a neuromuscular disease caused by the expansion of a CAG repeat in the *androgen receptor* (*AR*) gene. Mutant AR has been postulated to alter the expression of genes important for mitochondrial function and induce mitochondrial dysfunction. Here, we show that the expression levels of peroxisome proliferator-activated receptor-γ (PPARγ), a key regulator of mitochondrial biogenesis, were decreased in mouse and cellular models of SBMA. Treatment with pioglitazone (PG), an activator of PPARγ, improved the viability of the cellular model of SBMA. The oral administration of PG also improved the behavioral and histopathological phenotypes of the transgenic mice. Furthermore, immunohistochemical and biochemical analyses demonstrated that the administration of PG suppressed oxidative stress, nuclear factor-κB (NFκB) signal activation and inflammation both in the spinal cords and skeletal muscles of the SBMA mice. These findings suggest that PG is a promising candidate for the treatment of SBMA.

INTRODUCTION

Expansion of the trinucleotide CAG repeat in a coding region causes a group of neurodegenerative disorders including Huntington's disease that share several molecular pathomechanisms such as transcriptional dysregulation and mitochondrial dysfunction (1). Spinal and bulbar muscular atrophy (SBMA) is an adult-onset motor neuron disease that exclusively affects males and is caused by the expansion of a CAG repeat in the *androgen receptor* (*AR*) gene. Spinal and bulbar muscular atrophy is characterized by proximal muscle atrophy, weakness, fasciculations and bulbar involvement (2–4). No specific treatment for this disease has been identified. Previous studies showed that polyglutamine-expanded ARs accumulate in the nuclei of motor neurons in a testosterone-dependent manner and that the pathogenic AR perturbs the transcription of diverse genes that play important roles in the maintenance of neuronal function, thereby leading to neuronal dysfunction and the impairment of retrograde axonal transport in the mouse model of SBMA (5–8).

Recent studies have shown that the pathogenesis of SBMA is a result of both neurogenic and myopathic changes. Spinal and bulbar muscular atrophy patients present with extensive motor neuron loss together with signs of muscle degeneration, including the presence of central nuclei and the degeneration of fibers (3,9). The elevated levels of serum creatine kinase (CK) also support a myopathic pathogenesis in SBMA (10,11). Histopathological analyses of muscle tissues from the SBMA mice revealed both neurogenic and myopathic features (5,12–14). In the knock-in mouse model of SBMA, muscle degeneration occurs prior to the onset of spinal cord pathology (14). Furthermore, suppression of muscle pathology ameliorates motor

*To whom correspondence should be addressed at: Department of Neurology, Nagoya University Graduate School of Medicine, 65 Tsurumai-cho, Showa-ku, Nagoya 466-8550 Japan. Tel: +81 527442391; Fax: +81 527442394; Email: ka2no@med.nagoya-u.ac.jp (M.K.); Department of Neurology, Nagoya University Graduate School of Medicine, 65 Tsurumai-cho, Showa-ku, Nagoya 466-8550 Japan. Tel: +81 527442385; Fax: +81 527442384; Email: sobueg@med.nagoya-u.ac.jp (G.S.)

neuron degeneration in mouse models of SBMA, supporting the hypothesis that skeletal muscle is a primary target of polyglutamine-expanded-AR toxicity (13,15,16).

In the cellular model of SBMA, the accumulation of polyglutamine-expanded ARs in the presence of the relevant ligand results in mitochondrial membrane depolarization and an increase in the levels of reactive oxygen species that is blocked by treatment with the antioxidants co-enzyme Q10 and idebenone (17). Cytochrome *c* oxidase subunit Vb has been shown to interact with normal and mutant AR in a hormone-dependent manner, which may provide a mechanism for mitochondrial dysfunction in SBMA (18). Pathogenic ARs have also been shown to repress the transcription of subunits of peroxisome proliferator-activated receptor gamma coactivator-1 (PGC-1), a transcriptional co-activator that regulates mitochondrial biogenesis and function; this finding suggests that polyglutamine-mediated transcriptional dysregulation is associated with mitochondrial dysfunction (17). Mitochondrial dysfunction is a common pathomechanism of polyglutamine-mediated neurodegenerative disorders, and the transcriptional repression of PGC-1 caused by mutant huntingtin is also reported in Huntington's disease (19).

Peroxisome proliferator-activated receptor-γ (PPARγ) is a nuclear receptor and a ligand-activated transcription factor that regulates the expression of genes linked to a variety of physiological processes such as mitochondrial function, cell proliferation, atherosclerosis and immunity (20). Eicosanoids and 15-deoxy-prostaglandin J2 (15d-PGJ2) are naturally occurring PPARγ ligands, and thiazolidinediones, including pioglitazone (PG) and rosiglitazone, are synthetic PPARγ ligands. Thiazolidinediones elevate the expression levels of PPARγ in neuronal and non-neuronal cells and have been used to treat type II diabetes (21–23). Furthermore, transcript dysregulation of PPARγ has been shown in MN-1 cells that stably express mutant AR (AR-65Q) (17).

In the present study, we aimed to clarify whether PPARγ is involved in the pathogenesis of SBMA. Our results demonstrated that PPARγ is down-regulated in both the spinal cord and skeletal muscle of mice with SBMA and that the oral administration of a PPARγ agonist mitigates the neurodegeneration induced by polyglutamine-expanded ARs.

RESULTS

The expression level of PPARγ decreases in cellular models of SBMA

To examine the alteration in the PPARγ signaling pathway in SBMA model cells, we performed immunoblotting using neuronal cells (NSC34 cells) and muscular cells (C2C12 cells) transfected with a truncated AR (tAR-24Q or tAR-97Q). Immunoblotting analyses revealed that the expression levels of PPARγ were lower in tAR-97Q-transfected neuronal and muscular cells (tAR-97Q cells) than those in tAR-24Q-transfected cells (tAR-24Q cells), suggesting that the pathogenic AR protein bearing an expanded polyglutamine tract down-regulates the expression level of PPARγ (Fig. 1A–F). The expression levels of PPARγ were up-regulated by the administration of PG in NSC34 and C2C12 cells (Fig. 1A–F). On the other hand, the expression levels of AR were not altered by PG (Fig. 1A–F). Quantitative real-time polymerase chain reaction (RT-PCR) analyses showed that mRNA levels of PPARγ were lower in tAR-97Q cells of NSC34 and C2C12 cells than those in tAR-24Q cells; however, these levels were increased in cells treated with PG (Fig. 1A–F). Human neuroblastoma SH-SY5Y cells transfected with tAR-97Q had a lower luciferase activity under control of the *PPARγ* promoter compared with the cells transfected with tAR-24Q, indicating that the pathogenic AR inhibits the activity of the *PPARγ* promoter (Supplementary Material, Fig. S1A). SH-SY5Y cells, which stably express full-length AR-97Q also attenuated the activity of *PPARγ* promoter compared with the cells with full-length AR-24Q, and dihydrotestosterone (DHT) treatment intensifies this effect (Supplementary Material, Fig. S1B). These findings suggest that the decrease of PPARγ is associated with the nuclear accumulation of the pathogenic AR and that the transcriptional down-regulation of *PPARγ* by AR is, at least partially, hormone dependent. The expression levels of PPARγ in the spinal cords and skeletal muscles of autopsied specimens of SBMA patients had lower immunoreactivities to PPARγ than samples from control patients (Supplementary Material, Fig. S2A, B). We next investigated the effect of the increased expression of PPARγ on the cellular viability of tAR-97Q cells (Fig. 1G–L). The transient overexpression of PPARγ improved cellular viability and mitochondrial activity and attenuated cellular damage according to results of the lactate dehydrogenase (LDH) assay in both the NSC34 and C2C12 cells transfected with tAR-97Q. These findings led us to believe that the PPARγ agonist PG is a possible candidate for the treatment of SBMA.

Next, we analyzed the effects of PG on polyglutamine-mediated cytotoxicity in NSC34 and C2C12 cells by measuring cellular viability, cell death, Annexin V-positive cells, and LDH release. The transient overexpression of tAR-97Q resulted in diminished cellular viability and increased cell death, apoptotic cells and LDH release in NSC34 and C2C12 cells (Fig. 1M–T). Treatment with PG at a dose of 0.1 μM improved cellular viability of both cell lines (Fig. 1M, Q). Cell death, apoptotic cells and LDH release were also reduced by treatment with 0.1 μM PG (Fig. 1N–P, R–T). Cellular viability and cytotoxicity assays using primary cortical neurons showed similar findings (Supplementary Material, Fig. S3A, B). We further confirmed the beneficial effects of PG on hormone-dependent pathogenesis in SBMA. Pioglitazone improved the cell viability and attenuates apoptosis of a cellular model of SBMA, which stably expresses full-length AR-97Q and was treated with DHT (Supplementary Material, Fig. S4A, B). In contrast, the knock-down of PPARγ via RNAi increased LDH release and decreased mitochondrial activity in the NSC34 and C2C12 cells (Supplementary Material, Fig. S5A–C). Moreover, the effect of PG treatment was not seen when PPARγ was knocked-down, indicating that the neuroprotection by PG is dependent on PPARγ. To confirm the beneficial effects of PG on neural function, we measured the length of the axons of treated and untreated NSC34 cells (Supplementary Material, Fig. S6A, B). The axons of tAR-97Q cells were shorter than those of tAR-24Q cells, and this phenotype was improved by treatment with 0.1 μM PG.

Pioglitazone improves the histopathological findings of the spinal cord and skeletal muscle of SBMA

To test the effects of PPARγ activation *in vivo*, PG was administered to 6-week-old SBMA (AR-97Q) transgenic mice at

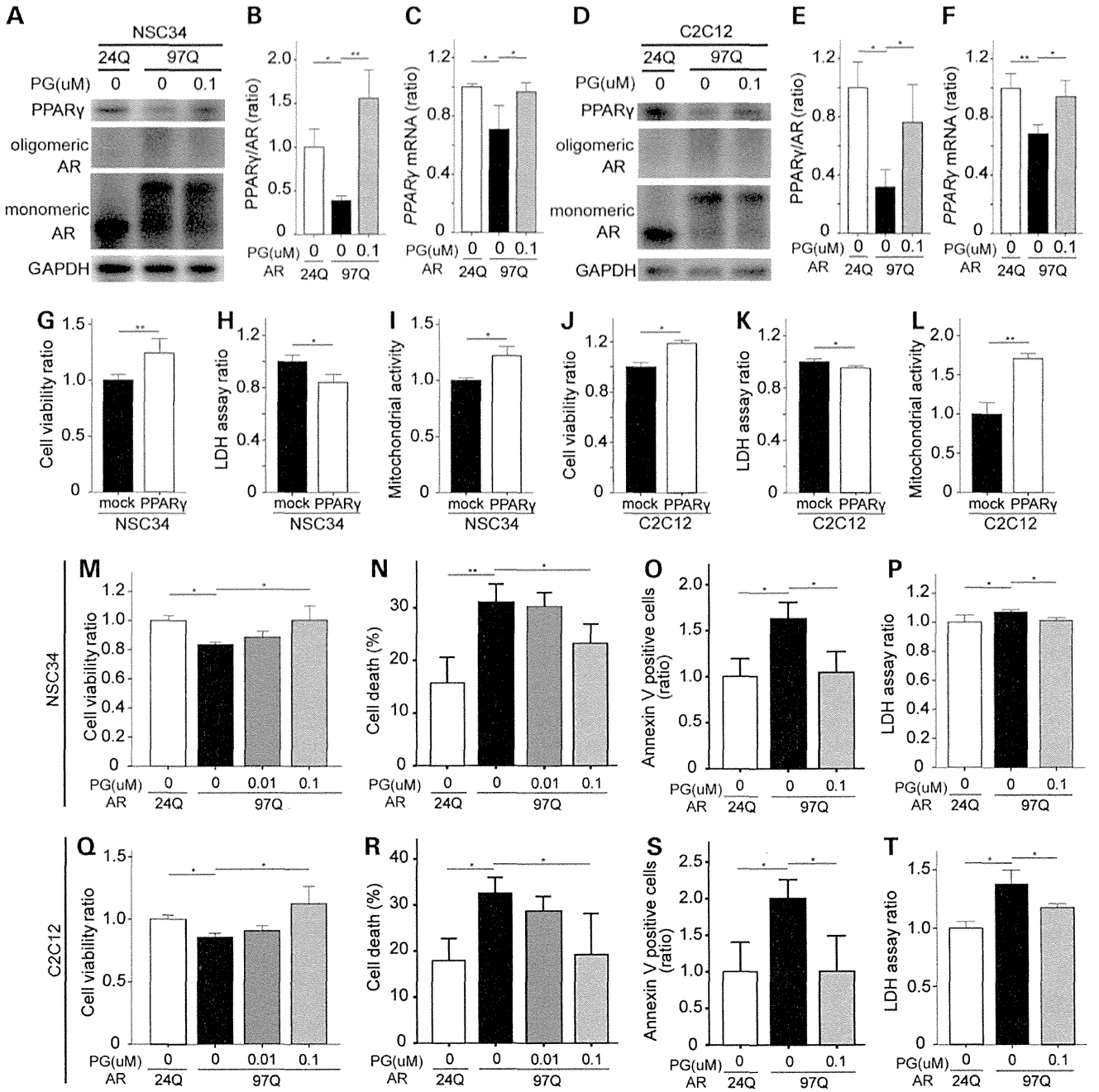

Figure 1. Pioglitazone (PG) improves the viability of cellular models of SBMA. (**A–F**) The protein and mRNA levels of *PPARγ* in NSC34 cells (A–C) and C2C12 cells (D–F) transfected with tAR-24Q or tAR-97Q and treated with or without PG. The ratio of PPARγ levels to monomeric and oligomeric AR levels (B, E). Quantitative analysis of PPARγ and AR was performed using densitometry. The *PPARγ* mRNA levels were measured using RT-PCR (C, F) ($n = 3$ per group). (**G–L**) The viability, LDH release and mitochondrial activity of NSC34 (G–I) and C2C12 cells (J–L) co-transfected with tAR-97Q and a mock or PPARγ vector ($n = 3$ per group). (**M–T**) The viability, cell death, Annexin V-positive cells and LDH release of NSC34 cells (M–P) and C2C12 cells (Q–T) transfected with tAR-24Q or tAR-97Q and treated with or without PG ($n = 6$ per group). Error bars indicate s.e.m. * $P < 0.05$ and ** $P < 0.01$ by unpaired *t*-test (G–L) or ANOVA with Dunnett's test (B, C, E, F, M–T).

concentrations of 0.01 and 0.02% in the feed until the end of analysis. No differences in feed intake were observed among the untreated, 0.01% PG-treated and 0.02% PG-treated mice at 8 weeks (data not shown). The AR-97Q mice fed the 0.02% PG-treated diet consumed 26.5 ± 1.04 mg/kg/day of PG at 8 weeks and 24.3 ± 4.44 mg/kg/day at 12 weeks. The oral administration of 0.02% PG from 6 weeks of age onward improved the body weight, performance on the rotarod task, grip power and lifespan of AR-97Q mice, although PG administered at a 0.01% dose did not improve the AR-97Q phenotype (Fig. 2A–D). Pioglitazone at 0.02% also limited the muscle atrophy and improved the stride length of the AR-97Q mice

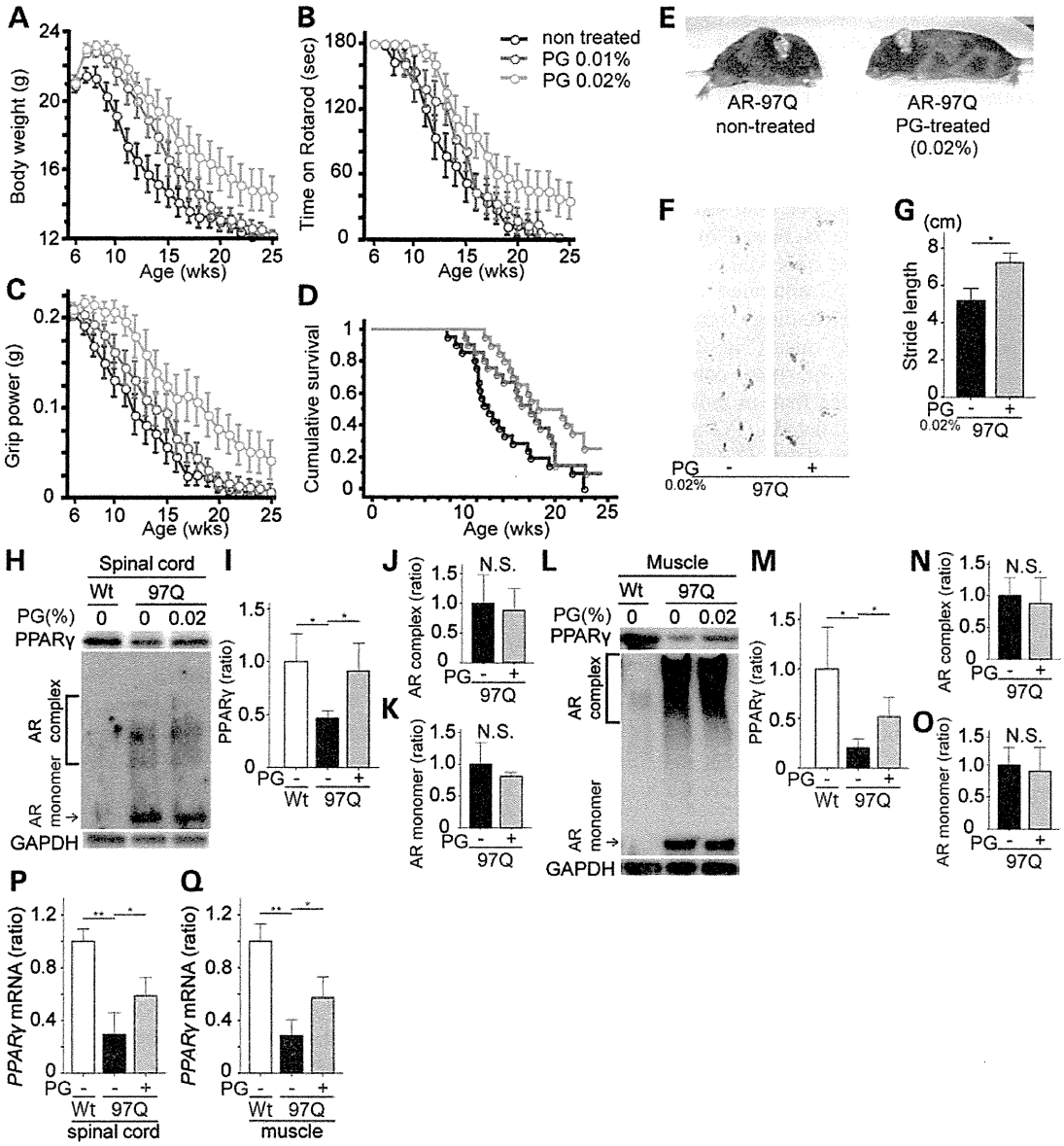

Figure 2. Pioglitazone alleviates neuromuscular phenotypes of SBMA mice. (**A**–**D**) Body weight (A), rotarod performance (B), grip power (C) and survival rate (D) of PG-treated AR-97Q mice ($n = 22$ for 0.01% PG and $n = 20$ for 0.02% PG) and untreated AR-97Q mice ($n = 21$). All parameters improved after treatment with PG at a dose of 0.02% ($P < 0.05$ at 13 weeks by ANOVA with Dunnett's test for body weight, rotarod performance and grip power; and $P < 0.005$ by log-rank test). (**E**) Muscle atrophy of 13-week-old AR-97Q mice treated with or without PG. (**F**) Footprints of 13-week-old AR-97Q mice. Front paws are shown in red, and hind paws are shown in blue. (**G**) Quantification of the footprints (13 weeks old) ($n = 3$ per group). (**H**–**Q**) Immunoblots for AR and PPARγ of the spinal cords (H–K) and skeletal muscles (L–O) of 13-week-old mice. Quantitative analysis was performed using densitometry ($n = 3$ per group). (P, Q) The mRNA levels of *PPARγ* in the spinal cord (P) and skeletal muscle (Q) of 13-week-old mice were measured using RT-PCR ($n = 3$ per group). Error bars indicate s.e.m. $^{*}P < 0.05$ and $^{**}P < 0.01$ by unpaired *t*-test (G, J, K, N, O) or ANOVA with Dunnett's test (I, M, P, Q). N.S., not significant.

(Fig. 2E–G). On the other hand, the administration of 0.02% PG had no detectable effects on the phenotypes of wild-type mice (Supplementary Material, Fig. S7A–D). There was a tendency that wild-type mice treated with PG gained weight compared with untreated wild-type mice, although the difference was not statistically significant (Supplementary Material, Fig. S7A–D). On the other hand, PG treatment increased the amount of food intake of the wild-type mice at the beginning of the treatment, but this effect faded with aging: 132.6 ± 2.5 mg/g/day of the diet without PG, and 148.5 ± 2.3 mg/g/day of the 0.02% PG-treated diet at 8 weeks ($P < 0.05$ by unpaired *t*-test); 118.2 ± 5.0 mg/g/day of the diet without PG, and 108.8 ± 10.4 mg/g/day of the 0.02% PG-treated diet at 12 weeks ($P > 0.05$).

We also examined the effects of PG when the administration was initiated after the onset of neurological symptoms. The oral administration of 0.02% PG from 8 weeks of age onward improved the body weight, performance on the rotarod task, grip power and lifespan of AR-97Q mice; however, its effects on survival were weaker than those observed when the treatment was initiated at 6 weeks of age. Specifically, the lifespan of the

mice treated at 6 and 8 weeks was 52.9 and 31.5% longer, respectively, than that of the untreated AR-97Q mice (Supplementary Material, Fig. S8A–D).

Next, we examined the biological effects of PPARγ-targeted therapy on AR-97Q mice. In agreement with the results of the cellular experiments, quantitative analyses using densitometry revealed that the expression levels of PPARγ were lower in spinal cords of untreated AR-97Q mice than those of wild-type mice; however, these levels were increased by PG treatment (Fig. 2H, I). Little difference was observed in the expression levels of AR in spinal cords of untreated and PG-treated AR-97Q mice (Fig. 2J, K). Similar findings were also observed in the skeletal muscle of AR-97Q mice (Fig. 2L–O). *PPARγ* mRNA levels were also lower in the spinal cords and skeletal muscles of untreated AR-97Q mice than in those of wild-type mice; these levels were also up-regulated in PG-treated AR-97Q mice (Fig. 2P, Q). The mRNA levels of *PGC1α* in the spinal cord were lower in untreated AR-97Q mice than those in wild-type mice. Although not significant, there was a trend that PG treatment increases the mRNA level of *PGC1α* in the spinal cord of AR-97Q mice (Supplementary Material, Fig. S9).

To investigate the pathological changes underlying the change in phenotype induced by PG, we performed immunohistochemistry on the spinal cords and skeletal muscles of wild-type, untreated AR-97Q and PG-treated AR-97Q mice. The number of 1C2-positive cells in the spinal cords and skeletal muscles was not significantly different between untreated and PG-treated AR-97Q mice (Fig. 3A–D). Immunohistochemistry for choline acetyltransferase (ChAT) in the anterior horn of the spinal cord revealed that motor neurons were atrophied in untreated AR-97Q mice but not in wild-type mice; however, the neurons were larger in PG-treated AR-97Q mice (Fig. 3E, F). Immunoreactivity to ChAT was also restored by PG treatment. Hematoxylin and eosin staining demonstrated that skeletal muscle fibers were atrophied in untreated AR-97Q mice and that PG treatment mitigated the amyotrophy in AR-97Q mice (Fig. 3G, H). Immunohistochemistry analyses using an antibody against glial fibrillary acid protein (GFAP—a marker of reactive astrogliosis) detected increased immunoreactivity in the anterior horn of the spinal cord of untreated AR-97Q mice; however, astrogliosis was attenuated by PG treatment (Fig. 3I, J). PPARγ immunohistochemistry in the spinal cord and skeletal muscle revealed that the signal intensity of PPARγ in the motor neurons and skeletal muscles was down-regulated in untreated AR-97Q mice and up-regulated by PG treatment (Supplementary Material, Fig. S10A–D). To evaluate the side effects of PG, blood was collected from the mice at 13 weeks to measure CK, aspartate aminotransferase, alanine aminotransferase and LDH serum levels. No abnormal values were observed in PG-treated AR-97Q mice, indicating that the oral administration of 0.02% PG did not induce systemic adverse effects (Supplementary Material, Fig. S11A–D). Fasting blood glucose levels were not significantly different among wild-type, untreated AR-97Q and PG-treated AR-97Q mice (Supplementary Material, Fig. S11E).

Pioglitazone suppresses oxidative stress in SBMA mice

Rosiglitazone, another PPARγ agonist, has been reported to prevent mitochondrial dysfunction and oxidative stress in mutant huntingtin-expressing cells (24). We therefore investigated the effects of PG on oxidative stress to understand the molecular basis of neuronal and muscular protection conferred by PG. We measured the mitochondrial activity of NSC34 cells and C2C12 cells that were transfected with tAR-24Q or tAR-97Q and treated with or without PG (Fig. 4A, B). The mitochondrial activity of tAR-97Q cells was lower than that of tAR-24Q cells and was improved by treatment with 0.1 μM PG.

We next measured the activity of cytochrome *c* oxidase (CCO—a marker of mitochondrial function) in the skeletal muscles of AR-97Q mice (Fig. 4C). In total, 1.5–3.0% of fibers were negative for CCO in untreated AR-97Q mice; in contrast, almost no CCO-negative fibers were found in wild-type or PG-treated AR-97Q mice ($P < 0.05$ by ANOVA with Dunnett's test for CCO-negative fibers in untreated AR-97Q mice compared with wild-type or PG-treated AR-97Q mice). To examine the expression levels of proteins related to oxidative stress, we performed immunohistochemistry using antibodies against nitrotyrosine and 8-hydroxy-2′-deoxyguanosine (8-OHdG) in the spinal cords and skeletal muscles of 13-week-old mice (Fig. 4D–G). The immunoreactivity to nitrotyrosine (a marker of oxidated protein) in the motor neurons and skeletal muscles was higher in untreated AR-97Q mice than that in wild-type mice; however, the intensity was lowered after PG treatment (Fig. 4D, E). Similar effects were also observed for 8-OHdG, a marker of oxidative stress in nucleic acids (Fig. 4F, G). Specifically, PG limited the levels of nuclear 8-OHdG, particularly in motor neurons (Fig. 4F, G). We next examined the daily urinary 8-OHdG excretion of 13-week-old mice (Fig. 4H) and found that 8-OHdG excretion was higher in untreated AR-97Q mice than that in wild-type mice and was lowered by PG treatment. In a similar manner, the urinary 8-OHdG levels of SBMA patients were reported to be significantly higher than those of control patients and strongly correlated with motor function scores (25). Furthermore, immunoblot analyses using anti-4-hydroxy-2-nonenal (HNE) antibodies in the spinal cords and skeletal muscles of 13-week-old mice revealed that the expression levels of HNE, a marker of lipid peroxidation chain reactions, in the spinal cord and skeletal muscle of untreated AR-97Q mice were up-regulated and suppressed by PG treatment (Fig. 4I–K). These results suggest that PG alleviates the oxidative stress that appears to underlie the pathogenesis of SBMA.

Pioglitazone suppresses the activation of nuclear factor-κB (NFκB) pathway in SBMA mice

Nuclear factor-κB is a nuclear transcription factor that regulates the expression of a large number of genes that are critical for the regulation of apoptosis, viral replication, tumorigenesis, inflammation and various autoimmune disorders. Previous studies have demonstrated that PG exerts anti-inflammatory effects via the attenuation of NFκB activation in the central nervous system (26,27). The augmented expression of NFκBp50 and NFκBp65 in NSC34 cells and C2C12 cells decreased cellular viability and mitochondrial activity and increased cellular damage (Supplementary Material, Fig. S12A–D). The nuclei of spinal motor neurons and skeletal muscles in autopsied specimens of SBMA patients showed increased levels of immunoreactivity to NFκB relative to control patients (Supplementary Material, Fig. S13A, B). To evaluate the activity of the NFκB pathway in cellular and mouse models of SBMA, we performed

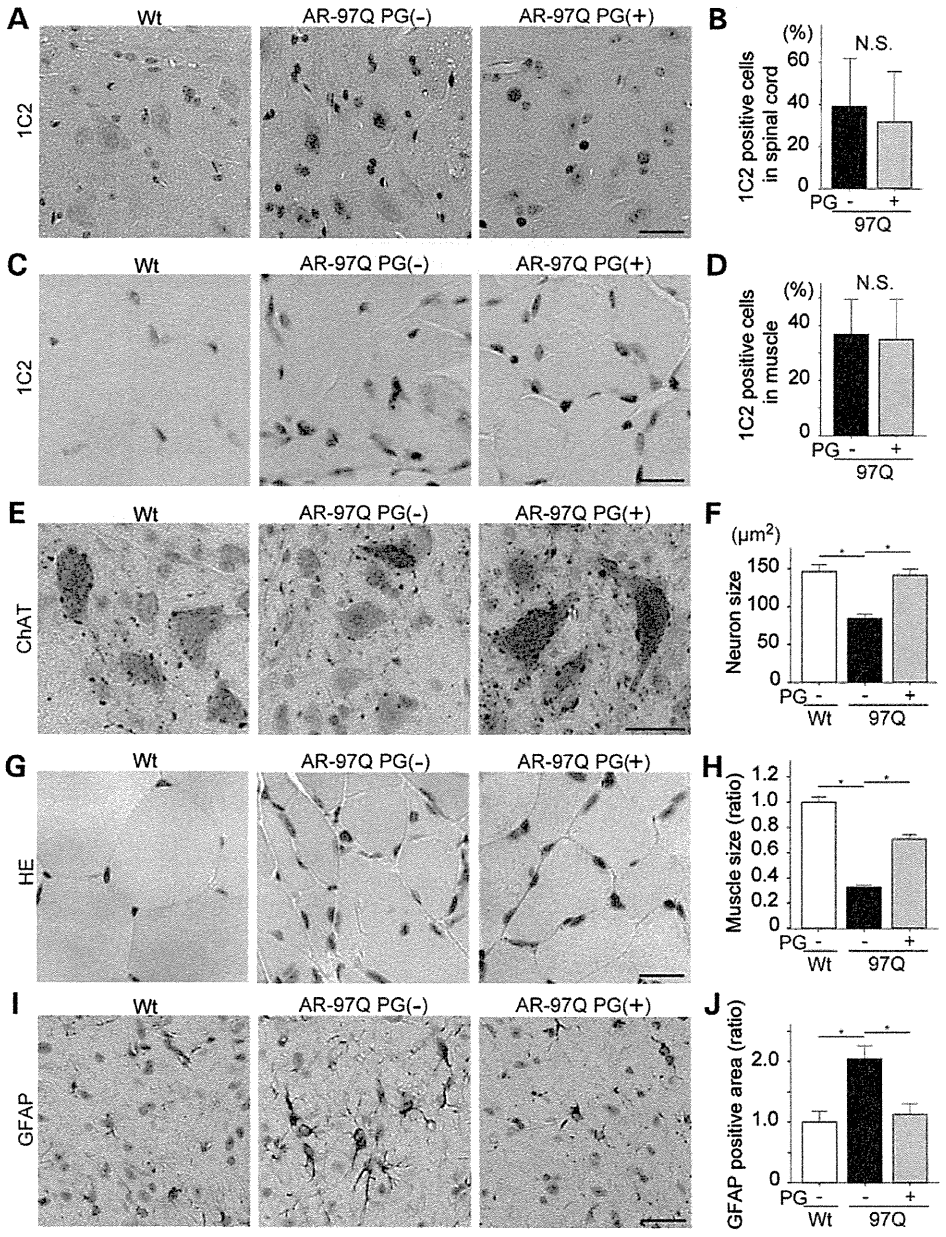

Figure 3. Effect of PG on the histopathology of SBMA mice. (**A**–**D**) Immunohistochemistry with quantitative analyses for 1C2 (an anti-polyglutamine antibody) in 13-week-old mice. (**E, F**) Anti-ChAT immunostaining of 13-week-old mice. (**G, H**) Hematoxylin and eosin staining of the skeletal muscles (G) and quantitation of muscle fiber size (H) in 13-week-old mice. (**I, J**) Immunohistochemistry with quantitative analysis for GFAP (a marker of reactive astrogliosis) in 13-week-old mice. Quantitative analyses were performed with $n = 3$ per group. Error bars indicate s.e.m. Statistical analyses were performed using the unpaired *t*-test (B, D). $^*P < 0.01$ by ANOVA with Dunnett's test (F, H, J). N.S., not significant. Scale bars: 25 μm (A, C, E, G, I).

immunoblotting for nuclear NFκBp65, cytoplasmic inhibitory protein-κ-Bα (IκBα) and phosphorylated IκBα (pIκBα) in NSC34 and C2C12 cells that were transfected with tAR-24Q or tAR-97Q and treated with or without PG. The expression levels of nuclear NFκBp65 and cytoplasmic pIκBα were up-regulated in untreated tAR-97Q cells compared with tAR-24Q cells but were down-regulated by PG treatment (Fig. 5A–H). The expression level of cytoplasmic IκBα was not significantly different among tAR-24Q, untreated tAR-97Q and PG-treated tAR-97Q cells. Anti-NFκBp65 and pIκBα immunohistochemistry also showed that the immunoreactivities of the spinal motor neurons and skeletal muscles were higher in untreated AR-97Q mice than those in wild-type mice and lower in the PG-treated AR-97Q mice (Fig. 6A–D). The alteration of NFκB signaling shown in cellular models was also observed in immunoblot analyses of spinal cords and skeletal muscles in 13-week-old wild-type untreated AR-97Q and PG-treated AR-97Q mice (Fig. 6E–L). These findings suggest that PG inhibits the activity of the NFκB pathway in both the spinal cord and skeletal muscle of AR-97Q mice.

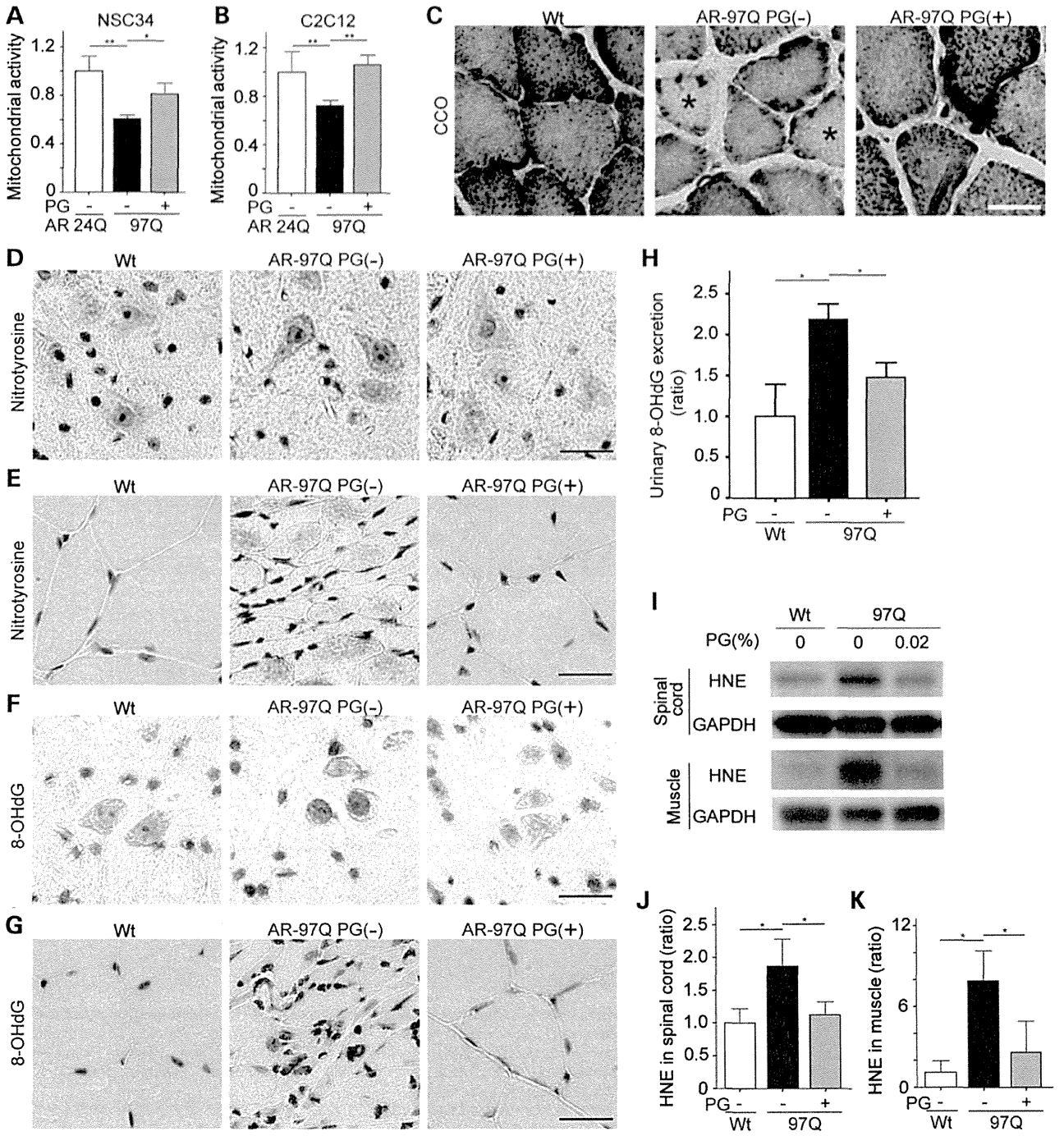

Figure 4. Effect of PG on oxidative stress in cellular and mouse models of SBMA. (**A, B**) Mitochondrial activity of the NSC34 (A) and C2C12 cells (B) transfected with tAR-24Q or tAR-97Q and treated with or without PG. (**C**) CCO (cytochrome *c* oxidase) staining of the skeletal muscles. Asterisks indicate CCO-negative muscle fibers. (**D–G**) Immunohistochemistry for nitrotyrosine and 8-OHdG in 13-week mice. (**H**) Quantitative analysis of the 24-h urinary 8-OHdG excretion of 13-week-old mice ($n = 3$ per group). Data are shown as ratio to urinary creatinine. (**I**) Immunoblots for 4-hydroxy-2-nonenal (HNE) in the spinal cords and skeletal muscles of 13-week-old mice. (**J, K**) Quantitative analysis of HNE in the spinal cords (J) and skeletal muscles (K) ($n = 3$ per group) using densitometry. Error bars indicate s.e.m. $^{*}P < 0.05$ and $^{**}P < 0.01$ by ANOVA with Dunnett's test (A, B, H, J, K). Scale bars: 25 μm (D–G).

Effects of PG on microglia

PPARs also act as master regulators governing the polarization of macrophages and microglia into 'M2' or 'alternative' activation states that suppress inflammation and promote phagocytosis and tissue repair (28,29). In contrast, microglia in 'M1' or 'classical' activation states promote the formation of the extremely toxic compound peroxynitrite, which causes damage

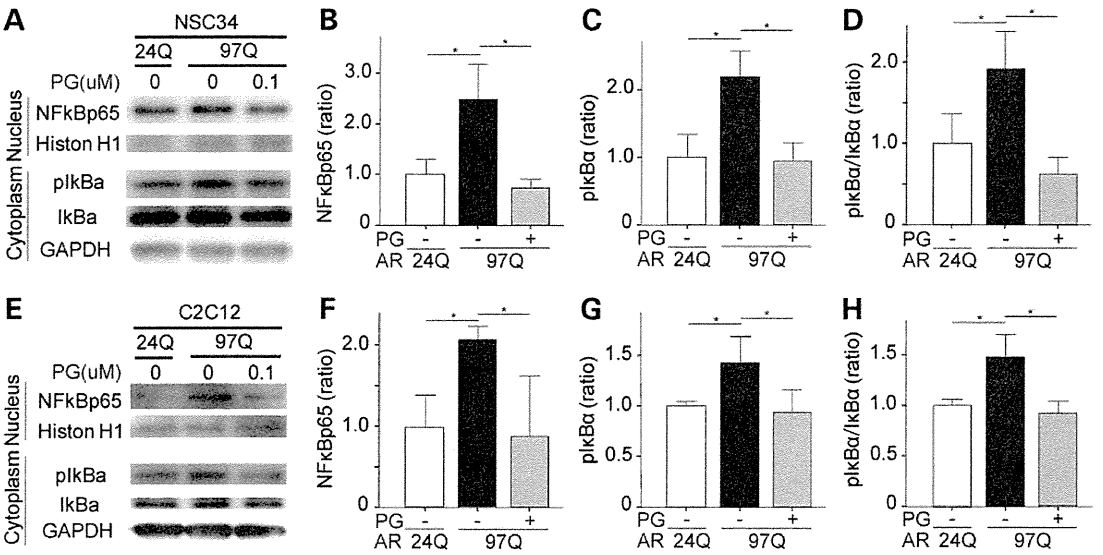

Figure 5. Effect of PG on NFκB signals in cellular model of SBMA. (**A**–**H**) Immunoblots of nuclear NFκBp65, cytoplasmic pIκBα and IκBα in NSC34 (A–D) and C2C12 cells (E–H) transfected with tAR-24Q or tAR-97Q and treated with or without PG. Quantitative analyses were performed using the densitometry of NFκBp65 (B, F), pIκBα (C, G) and the ratio of pIκBα to IκBα (D, H) ($n = 3$ per group). Error bars indicate s.e.m. * $P < 0.05$ by ANOVA with Dunnett's test (B–D, F–H).

to healthy tissue. Therefore, we investigated the state of microglia and the effects of PG on these cells in AR-97Q mice. Immunohistochemical analyses showed that cells in the anterior horn of the spinal cords of untreated AR-97Q mice had more microglia that were positive for CD86, an M1 glial cell surface marker, than the corresponding cells in wild-type mice; however, this phenomenon was mitigated by PG treatment (Fig. 7A, B). In contrast, PG increased immunoreactivity against Arg1, an M2 glial marker, in the microglia of the anterior horn of the spinal cords of AR-97Q mice; untreated AR-97Q mice had decreased immunoreactivities to Arg1 (Fig. 7C, D). Immunohistochemistry using anti-Iba1, a general microglial marker, demonstrated little difference in the levels of this marker among wild-type, untreated AR-97Q and PG-treated AR-97Q mice (Fig. 7E, F). Similar findings were observed in immunoblot analyses of the anterior part of the spinal cords of 13-week-old mice (Fig. 7G–J). The M1/M2 ratio was therefore markedly higher in the microglia of the anterior horn of the spinal cords of untreated AR-97Q mice than in those of wild-type mice. However, the M1/M2 ratio was restored to normal levels by PG treatment, suggesting that the release of proinflammatory molecules is associated with the pathogenesis of SBMA. In addition, PG treatment induced the phenotypic conversion of microglia from a proinflammatory M1 state to an anti-inflammatory M2 state, which is associated with neuroprotection. The results of immunohistochemical analyses revealed that there were more CD86-positive macrophages in the skeletal muscles of untreated AR-97Q mice than those of wild-type mice, and this phenomenon was suppressed by PG treatment (Supplementary Material, Fig. S14A). In contrast, PG increased the number of Arg1-positive macrophage in the skeletal muscles of AR-97Q mice; untreated AR-97Q mice had less immunoreactivities to Arg1 compared with wild-type mice (Supplementary Material, Fig. S14B).

The expression of genes related to inflammation is significantly altered in the spinal cord and muscle of PG-treated AR-97Q mice

To understand the global molecular changes induced by the administration of PG, we prepared total mRNA samples from the spinal cords and skeletal muscles of 13-week-old untreated AR-97Q and PG-treated AR-97Q mice and performed gene expression analyses. The microarray analyses found that the expression levels of 83 genes and 422 genes were significantly increased (>2-fold and >3-fold, respectively) in the spinal cords and skeletal muscles, respectively, of PG-treated mice ($P < 0.05$) (Supplementary Material, Fig. S15, S16). We then performed functional analysis using gene ontology (GO) of these genes, classifying them into several functional categories: immune response, extracellular matrix, cell adhesion, metabolism and others (Fig. 8A, B). As for the down-regulated genes, there were no GO terms, the frequency of which was found to be significantly decreased (less than one-half in the spinal cords and less than one-third in the skeletal muscles). Genes related to the immune response and extracellular matrix were predominantly altered by PG treatment, suggesting that the PPARγ agonist modulates the inflammatory response (especially along the NFκB pathway). The results also demonstrated that genes from similar functional categories are found in the spinal cord and skeletal muscle, indicating that PG attenuates the toxicity of polyglutamine-expanded AR in both neural and muscular tissues via a similar mechanism (Supplementary Material, Fig. S17A, B).

DISCUSSION

Recent studies have shown that mitochondrial dysfunction and oxidative stress-mediated neuronal toxicity are implicated in

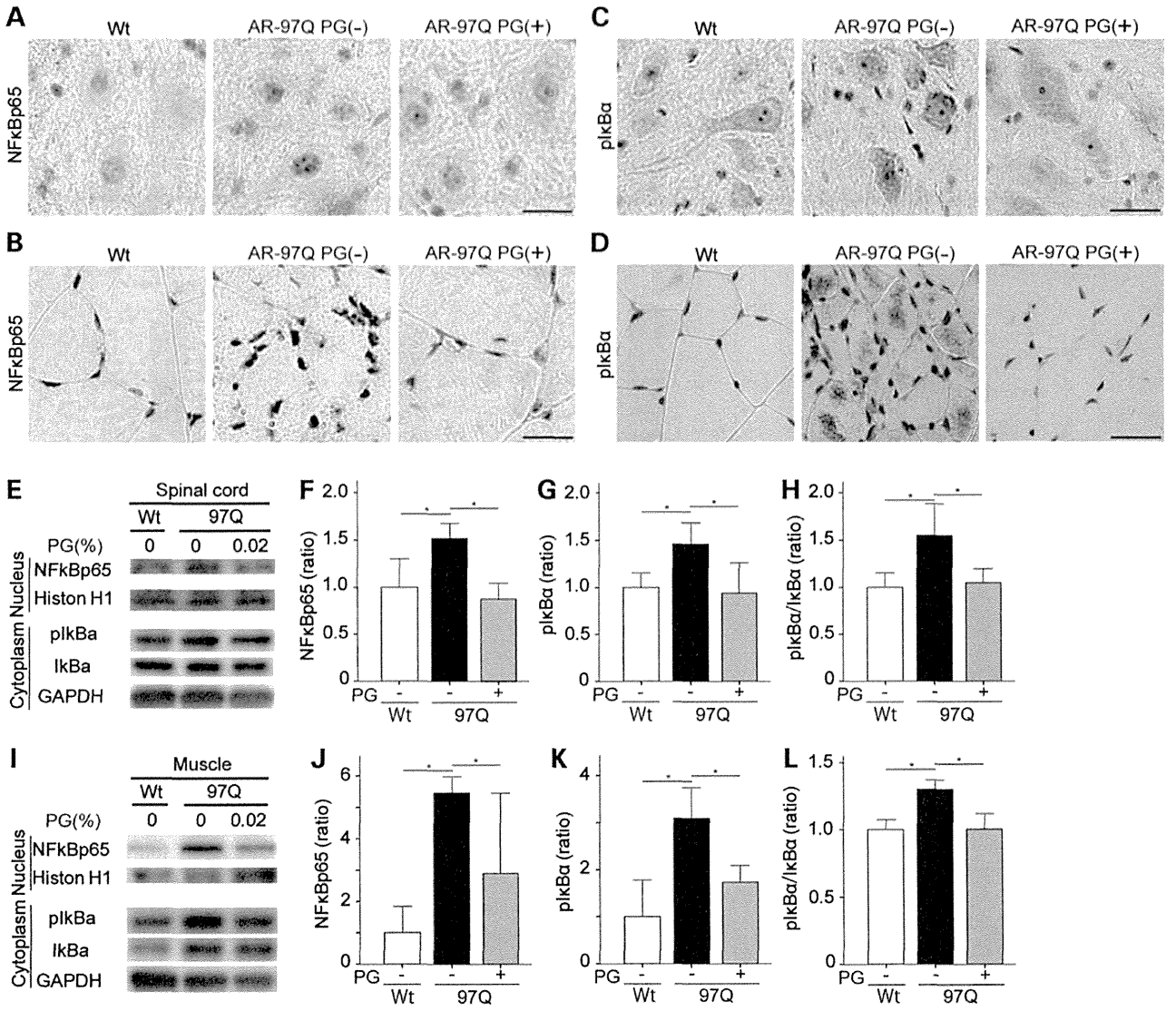

Figure 6. Effect of PG on NFκB signals of SBMA mice. (**A–D**) Immunohistochemistry for NFκBp65 (A, B) and pIκBα (C, D) in 13-week-old mice. (**E–L**) Immunoblots for nuclear NFκBp65, cytoplasmic pIκBα and IκBα in the spinal cords (E–H) and skeletal muscles (I–L) of 13-week-old mice. Quantitative analyses were performed using the densitometry of NFκBp65 (F, J), pIκBα (G, K) and the ratio of pIκBα to IκBα (H, L) ($n = 3$ per group). Error bars indicate s.e.m. * $P < 0.05$ by ANOVA with Dunnett's test (F–H, J–L). Error bars indicate s.e.m. * $P < 0.05$ by ANOVA with Dunnett's test (F–H, J–L). Scale bars: 25 μm (A–D).

various neurodegenerative diseases, including Huntington's disease, amyotrophic lateral sclerosis (ALS) and Friedreich's ataxia (30–35). In the present study, we demonstrated that the mRNA and protein levels of PPARγ, a regulator of mitochondrial function, were decreased in mouse and cellular models of SBMA. The results of reporter assay showed that the pathogenic AR suppressed the activity of *PPARγ* promoter. The mRNA levels of PGC1α, the co-activator of PPARγ, were also down-regulated in the spinal cord of our mouse model of SBMA, as reported in another mouse model of this disease (17). Decreased mRNA expression of PGC1α and PGC1α-regulated factors is also reported in the ALS mouse model and in human sporadic ALS, suggesting that mitochondrial dysfunction is a common pathological feature of motor neuron diseases (36,37). We also demonstrated that the overexpression of PPARγ and the administration of PG, a PPARγ agonist, improved the viability of cellular models of SBMA. Moreover, the oral administration of PG to SBMA mice improved neurological symptoms and histopathological findings. Pioglitazone mitigated oxidative stress, mitochondrial dysfunction and the activation of the NFκB pathway in mouse and cellular models of SBMA, providing a mechanistic basis for this treatment. In addition, PG modulated microglial populations in the spinal cord of the SBMA mice. These findings suggest that the PPARγ pathway can inhibit oxidative stress, the NFκB pathway and inflammation in SBMA.

PPARγ agonists have been proven effective in mouse and cellular models of neurodegenerative disorders, trauma and stroke (21,24,27,38–45). For example, PG has been shown to

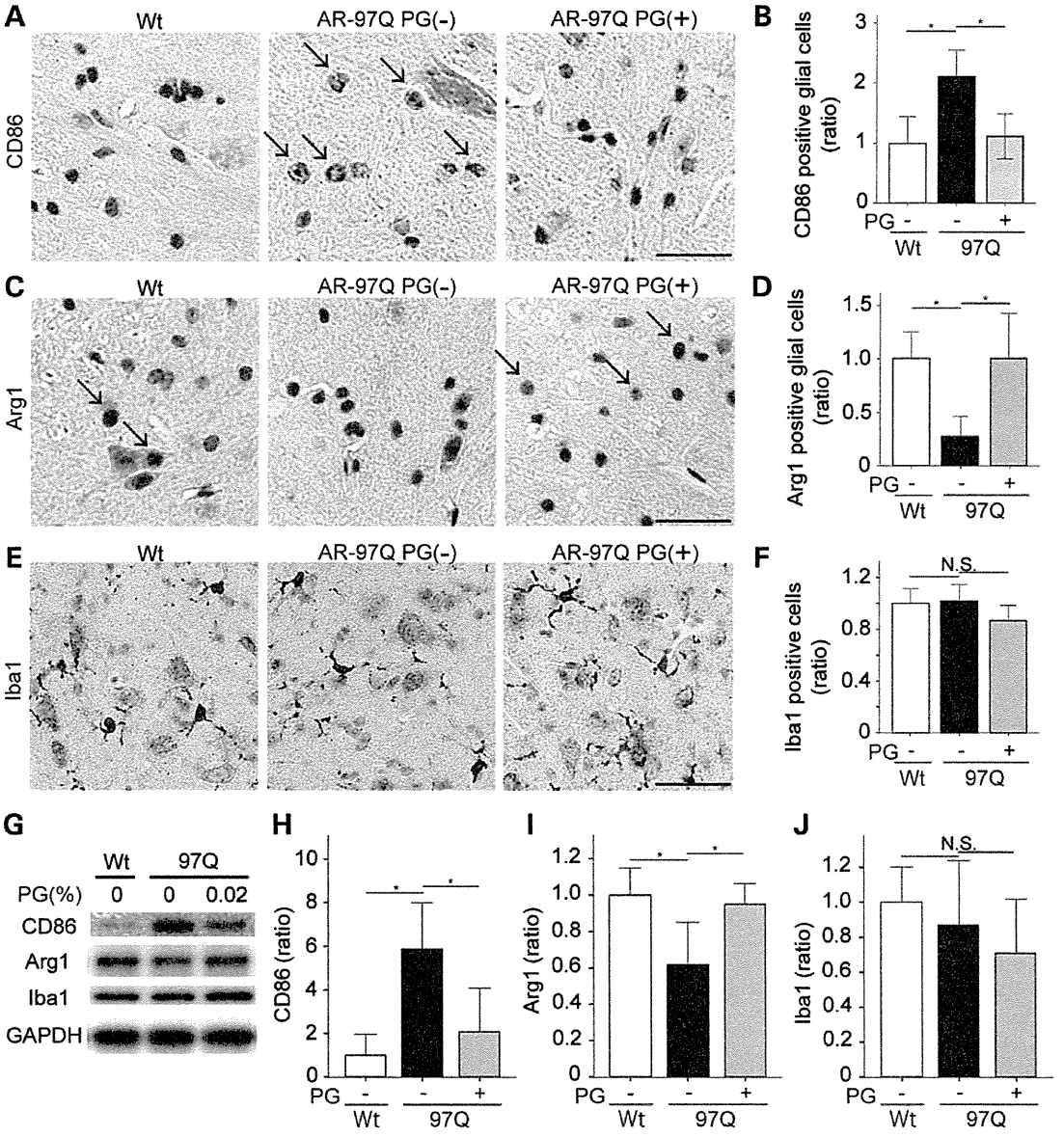

Figure 7. Effect of PG on the microglia of SBMA mice. (**A**–**F**) Immunohistochemistry with quantitative analyses of CD86 (A, B), Arg1 (C, D) and Iba1 (E, F) in 13-week-old mice. The arrows indicate the CD86- (A) and Arg1- (C) positive cells. Quantitative analyses of the ratio of CD86- (B), Arg1- (D) and Iba1- (F) positive cells in the anterior horn were performed with $n = 3$ per group. (**G**) Immunoblots for CD86, Arg1 and Iba1 in the anterior part of the spinal cord from 13-week-old mice. (**H**–**J**) Quantitative analysis using densitometry of CD86 (H), Arg1 (I) and Iba1 (J) ($n = 3$ per group). Error bars indicate s.e.m. $^*P < 0.05$ by ANOVA with Dunnett's test (B, D, F, H–J). N.S., not significant. Scale bars: 25 μm (A, C, E).

be neuroprotective in the G93A SOD1 transgenic mouse model of ALS (38), improving motor performance and increasing survival by reducing microglial activation and gliosis. Despite the promising preclinical trials using SOD1 mouse model, PG had no beneficial effects on the survival of ALS patients as add-on therapy to riluzole, indicating the difficulty of the translation from mouse models to human (46).

Pioglitazone has also been shown to reduce iNOS, NFκB and 3-nitrotyrosine immunoreactivity, and several of these findings were replicated in the present study. Pioglitazone treatment also improved motor function and mitigated oxidative stress and mitochondrial enzyme activity in a rat model of Huntington's disease induced by quinolinic acid (40). However, the administration of rosiglitazone to R6/2 transgenic Huntington's disease mice did not alter the course of survival or weight loss of the animals, possibly because insufficient levels of rosiglitazone were administered to sustain effective therapeutic levels or prevent rapid neurodegeneration (47).

Interestingly, in the present study, similar molecular changes related to oxidative stress and NFκB activation were observed in the motor neurons and skeletal muscles of SBMA mice. Microarray analyses showed that PG mitigated

A

GO term (spinal cord)	p value
collagen biosynthetic process	1.94E-03
collagen metabolic process	2.69E-03
proteinaceous extracellular matrix	2.69E-03
multicellular organismal macromolecule metabolic process	2.69E-03
multicellular organismal metabolic process	3.46E-03
extracellular matrix	4.12E-03
extracellular matrix structural constituent	4.37E-02

immune response
cell adhesion
extracellular matrix
metabolism

B

GO term (skeletal muscle)	p value
extracellular matrix	2.12E-28
extracellular region	1.20E-26
extracellular region part	1.66E-25
proteinaceous extracellular matrix	1.73E-25
extracellular space	2.29E-17
collagen	6.65E-16
extracellular matrix part	3.69E-14
fibrillar collagen	3.87E-08
extracellular matrix organization	2.44E-07
extracellular matrix structural constituent	2.44E-07
immune system process	2.44E-07
extracellular structure organization	2.53E-07
cell adhesion	9.29E-07
biological adhesion	1.18E-06
collagen fibril organization	1.93E-06
heparin binding	2.61E-06
glycosaminoglycan binding	3.26E-06
immune response	6.81E-06
protein heterotrimerization	1.80E-05
MHC class II protein complex	1.80E-05
carbohydrate derivative binding	1.83E-05
positive regulation of developmental process	5.89E-05
regulation of multicellular organismal process	5.89E-05
positive regulation of biological process	6.08E-05
antigen processing and presentation of exogenous peptide antigen	1.29E-04
antigen processing and presentation of exogenous peptide antigen via MHC class II	1.85E-04
sulfur compound binding	1.97E-04
plasma membrane part	2.24E-04
locomotion	3.93E-04
antigen processing and presentation of peptide antigen via MHC class II	4.06E-04
protein trimerization	4.06E-04
positive regulation of cellular process	4.49E-04
positive regulation of T cell activation	4.49E-04
antigen processing and presentation of exogenous	4.93E-04
antigen response to cytokine stimulus	6.29E-04
regulation of developmental process	7.18E-04
positive regulation of cell differentiation	7.18E-04
response to external stimulus	7.18E-04
antigen processing and presentation of peptide or polysaccharide antigen via MHC class II	7.18E-04
response to wounding	7.18E-04
cell activation	8.73E-04
regulation of defense response	9.11E-04
platelet-derived growth factor binding	9.29E-04
regulation of anatomical structure morphogenesis	9.32E-04
chemotaxis	9.77E-04

Figure 8. Gene ontology (GO) analysis. (**A**) The list of GO terms of the genes with expression levels that were significantly higher (>2-fold) in the spinal cords of PG-treated AR-97Q mice than in those of untreated AR-97Q mice at 13 weeks ($n = 3$ per group, $P < 0.05$). (**B**) The list of GO terms of the genes with significantly higher (>3-fold) expression levels in the skeletal muscles of PG-treated AR-97Q mice than in those of untreated AR-97Q mice at 13 weeks ($n = 3$ per group, $P < 0.05$).

these cellular events in both neuronal and muscular tissues. These effects were also observed in cellular experiments using neuronal and muscular cell lines. The results of the present study suggest that PG has direct effects on both neuronal and muscular degeneration in SBMA and that skeletal muscle is an important target for therapies that alleviate neuromuscular symptoms of SBMA.

Although we tested the ability of PG to modify mitochondrial function, our results also indicate that oxidative stress, the activation of the NFκB pathway and neuroinflammation play important roles in the pathogenesis of SBMA. Mitochondrial dysfunction, NFκB activation and the M1 microglial phenotype are known to be connected in several ways. For example, mitochondrial toxins caused by primary damage to the mitochondrial respiratory chain induce microglial activation and neuroinflammatory processes. Proinflammatory cytokines (such as tumor necrosis factor-α) released by M1 microglia alter the morphology and function of mitochondria (48,49). Furthermore, NFκB was recently identified as a physiological regulator of mitochondrial respiration, and NFκB-induced oxidative stress is thought to contribute to mitochondrial dysfunction in diabetic mice (50,51). NFκB activation in microglia also regulates inflammatory processes that exacerbate diseases such as ischemia and Alzheimer's disease (52). These findings implicate mitochondrial dysfunction, NFκB and microglial alteration in the pathogenesis of neurodegenerative diseases.

The results of the present study provide important insights into the NFκB-mediated pathogenesis of SBMA. The NFκB pathway was activated in the mouse and cellular models and in patients with SBMA. The overexpression of NFκBp50 or p65, key molecules of the signaling pathway, induced cellular damage in neuronal and muscular cells; however, PG treatment suppressed the activity of the NFκB pathway in the mouse and cellular models of SBMA. These findings suggest that NFκB signaling plays an important role in the pathogenesis of SBMA. NFκB activation has been implicated in the pathogenesis of various neurodegenerative disorders (35,53,54), and this pathway appears to be a commonly considered target of therapy for devastating neurological diseases.

Neuroinflammation is a common pathological feature of many neurodegenerative diseases and appears to play an important role in the non-cell autonomous pathogenesis (55,56) of several animal models of neurodegenerative disease. In animal models of ALS, lowering mutant superoxide dismutase 1 (SOD1) expression levels in microglia using the Cre–Lox recombination system significantly extended the survival of transgenic mice carrying a mutant human $SOD1^{G37R}$ gene (57–59). Moreover, microglia in the ALS mouse model appear to switch from an M2 state to an M1 state as the disease progresses (58,59). The present results suggest that PG exerts a neuroprotective effect on SBMA mice via the modulation of inflammation.

In conclusion, we demonstrated that PPARγ is down-regulated in SBMA and that the activation of this nuclear receptor by PG mitigates oxidative stress, NFκB activation and neuroinflammation and improves the symptoms and pathological findings of SBMA mice. Our results corroborate the decrease in PPARγ expression and the increases in oxidative stress and NFκB activity observed in autopsy samples from SBMA patients. Given that PG is already used as an oral-hyperglycemic drug and crosses the blood–brain barrier, this drug appears to be a safe and effective therapy for SBMA and other neurodegenerative diseases.

MATERIALS AND METHODS

Cell culture and transfection

Mouse NSC34 motor neuron-like cells (kindly provided by N.R. Cashman, University of British Columbia, Vancouver, Canada) and mouse C2C12 myoblast cells (DS Pharma Biomedical, Osaka, Japan) were cultured in a humidified atmosphere of 95% air/5% CO2 in a 37°C incubator in Dulbecco's Modified Eagle's Medium (DMEM) supplemented with 10% fetal bovine serum (FBS). DMEM/F12 with 10% FBS was used to culture SH-SY5Y human neuroblastoma cells (ATCC No. CRL-2266) and those stably expressing the human full-length AR-97Q. The plasmids were transfected using OPTI-MEM (Gibco, Germany) and Lipofectamine 2000 (Invitrogen, Carlsbad, CA, USA) according to the manufacturer's instructions. NSC34 cells were differentiated in DMEM for 96 h. Fetal horse serum (2%) was added to the medium for 48 h to differentiate the C2C12 cells. SH-SY5Y cells were differentiated in DMEM/F12 supplemented with 2% FBS and 20 μM retinoic acid. SH-SY5Y cells stably expressing AR-97Q were differentiated in DMEM/F12 supplemented with 20 μM retinoic acid and 1 nM 5α-dihydrotestosterone as described earlier (6).

Plasmid constructs and siRNA

The pEVRF-p65 vector encoding the murine RelA protein and the pCMV4-p50 vector encoding the NFκBp50 subunit were kindly provided by Drs. Genevieve Soucy and Jean-Pierre Julien (Department of Psychiatry and Neuroscience, Laval University, Research Centre of CHUL, Canada). The pcDNA3.1-PPARγ expression vector was cloned as previously described (60). The pCR3.1–AR–24Q and pCR3.1–AR–97Q plasmids were cloned as previously described (61). This truncated protein consisted of an N-terminal fragment of human *AR* containing 24 or 97 CAG repeats (1–645 bp and 1–864 bp, respectively) subcloned into pcDNA3.1 (6,62,63). To knock-down PPARγ, the following oligonucleotide siRNA duplexes were synthesized by Invitrogen and used to transfect the NSC34 and C2C12 cells: sense sequence, CAGAGCAAAGAGGUGGCCAUCCGAA; antisense sequence, UUCGGAUGGCCACCUCUUUGCUCUG. We used Stealth RNAi negative control duplex (Invitrogen) as the control siRNA. The NSC34 and C2C12 cells were transfected with the siRNA oligonucleotide duplex using Lipofectamine 2000 (Invitrogen) according to the manufacturer's instructions.

Cell viability, toxicity and apoptosis assays

The cell viability assays were performed using WST-8 (Roche Diagnostics, Mannheim, Germany). The cells were cultured in 24-well plates. Twenty-four hours after each treatment with the indicated concentrations of PG, the cells were incubated with the WST-8 substrate for 3–4 h and spectrophotometrically assayed at 450 nm using a plate reader (Powerscan HT, Dainippon Pharmaceutical, Osaka, Japan). The toxicity assays were performed using the Cytotoxicity Detection Kit PLUS (Roche Diagnostics, Indianapolis, IN). Twenty-four hours after the treatment, 100 μl of the medium was extracted from the plate and used for the assay. The medium was incubated with the substrate for 15 min and spectrophotometrically assayed at 490 nm using a plate reader. The number of dead cells was determined using a Countess cell counter (Invitrogen) after staining with trypan blue. For detecting apoptotic cells, we used Multi-Parameter Apoptosis Assay Kit (Cayman Chemical, MI, USA). The cells were cultured in 96-well black plates. After the treatment, plate reader fluorescence detection was performed according to the manufacturer's instructions.

Mitochondrial activity assay

The assessment of mitochondrial membrane potential was determined using MitoTracker™ green FM (Invitrogen) dyes. The dyes passively diffuse across the plasma membrane and accumulate in active mitochondria, whose accumulation is dependent upon membrane potential. The cells were incubated with 100 nM of the dyes for 30 min at 37°C in serum-free DMEM and washed with pre-warmed serum-free DMEM. The cells were then observed using a fluorescence microplate reader (Powerscan HT) at excitation and emission wavelengths of 490 and 516 nm, respectively.

Animals

AR-97Q (Line #7–8) male mice were bred and maintained as previously described (5,64). They have backcrossed at least 15 generations to C57BL/6 before used in the present study. The mice were genotyped by PCR using DNA from their tail (5). In the experiments, PG was administered at concentrations of 0.01 or 0.02% in the feed from 6 or 8 weeks of age until the end of the analysis, unless otherwise mentioned. Only males were used in this study. The litters were randomly allocated to PG-containing or normal chow. For pathological and biochemical analyses, the feed was administered to the mice beginning at 6 weeks of age.

Behavioral analysis

All of the tests were performed on a weekly basis, and the data were analyzed prospectively. The rotarod performance was assessed weekly using an Economex Rotarod (Ugo Basile, Comerio, Italy) as previously described (64). The grip strength was measured with a Grip Strength Meter (MK-380M, Muromachi Kikai, Tokyo, Japan) as described elsewhere (65).

Immunoblotting

Mice anesthetized with ketamine–xylazine were perfused with 4% paraformaldehyde fixative in phosphate buffer (pH 7.4). The tissues (whole brain, spinal cord, brainstem and skeletal muscle) were dissected and snap-frozen with powdered CO_2 in acetone. The tissues were homogenized in buffer containing 50 mM Tris–HCl (pH 8.0), 150 mM NaCl, 1% Nonidet P-40, 0.5% deoxycholate, 0.1% SDS and 1 mM 2-mercaptoethanol with Halt Protease and Phosphatase Inhibitor Cocktail (Thermo Scientific, Waltham, MA, USA) and centrifuged at 2500 × *g* for 15 min. The cultured cells were also lysed in the same reagent after intervention. NE-PER Nuclear Cytoplasmic Reagents (Thermo Scientific) were used for the analysis of the NFκB pathway. Equal amounts of protein were separated by 5–20% SDS–PAGE gels and transferred to Hybond-P membranes (GE Healthcare, Piscataway, NJ, USA). Primary antibody binding

was probed with horseradish peroxidase-conjugated secondary antibodies at a dilution of 1 : 5000, and the bands were detected using an immunoreaction enhancing solution (Can Get Signal; Toyobo, Osaka, Japan) and enhanced chemiluminescence (ECL Prime; GE Healthcare). An LAS-3000 imaging system (Fujifilm, Tokyo, Japan) was used to produce digital images. The signal intensities of these independent blots were quantified using IMAGE GAUGE software version 4.22 (Fuji) and expressed in arbitrary units. The membranes were reprobed with an anti-GAPDH (MAB374, 1 : 5000; Santa Cruz) antibody or Histone H1 (#05-457, 1 : 1000; Millipore, Billerica, MA, USA) for normalization.

Histology and immunohistochemistry

The mouse tissues were dissected, post-fixed in 10% phosphate-buffered formalin and processed for paraffin embedding. The sections to be stained with the anti-polyglutamine antibody (1C2) were treated with formic acid for 5 min at room temperature. The sections to be incubated with the anti-ChAT, GFAP, nitrotyrosine, pIκBα and Iba-1 antibodies were boiled in 10 mM citrate buffer for 15 min. The specificity of the monoclonal antibody against 8-OHdG (N45.1) has been characterized in a previous study (66). The sections to be incubated with the anti-8OHdG antibody were boiled in 0.1 M glycine buffer (pH 2.2) for 15 min. The sections to be incubated with an anti-NFκBp65 antibody were autoclaved using the 2100-Retriever (Funakoshi Corporation, Tokyo, Japan). Primary antibody binding was probed with a secondary antibody labeled with a polymer as part of the Envision+ system containing horseradish peroxidase (Dako Cytomation, Gostrup, Denmark). The immunohistochemical sections were photographed with an optical microscope (Axio Imager M1, Carl Zeiss AG, Göttingen, Germany). The immunoreactivity and cell sizes were analyzed with WinROOF (Mitani, Tokyo, Japan). The means ± s.e.m. were expressed in arbitrary units. For hematoxylin and eosin (H&E) staining, 6-μm-thick cryostat sections of the gastrocnemius muscles were air-dried and stained.

Quantitative analysis of immunohistochemistry

To assess 1C2-, CD86-, Arg1- and Iba1-positive cells, at least 50 consecutive 6-μm-thick axial sections of the thoracic spinal cord and skeletal muscle were prepared, and every fifth section was immunostained with each antibody. The numbers of 1C2-positive cells were counted in all of the neurons of the anterior horn of the 10 axial sections from the thoracic spinal cord of each group of mice ($n = 3$) under a light microscope (Bx51; Olympus, Tokyo, Japan). For the purposes of counting, we defined a motor neuron by its presence within the anterior horn and the obvious nucleolus in a given 6-μm-thick section. The numbers of 1C2-positive cells in skeletal muscles were calculated for >500 fibers in randomly selected areas of the 10 axial sections. To quantify the expression levels of nitrotyrosine, 8OHdG, NFκBp65 and pIκBα, we performed immunohistochemistry on every fifth section of the 25 consecutive sections. We measured the intensity of nuclear immunoreactivities for 8OHdG and NFκBp65 and the intensity of the cytoplasmic immunoreactivities for nitrotyrosine and pIκBα in the thoracic anterior horn of the 5 axial sections and in >500 cells in 5 randomly selected ×400 microscopic fields of the 5 sections of skeletal muscles from each group of mice ($n = 3$). We calculated the intensities by multiplying the staining concentration by cell sizes or nuclear sizes, which were quantified with WinROOF. To quantify the size of the motor neurons and the region of anti-GFAP immunoreactivity in the spinal anterior horn, we analyzed every fifth section of the 25 consecutive 6-μm-thick axial sections from the thoracic spinal cord using an image analyzer (WinROOF). To calculate the cell size of the skeletal muscles, >500 H&E stained fibers in randomly selected areas were examined using an image analyzer (WinROOF).

Cytochrome *c* oxidase staining of skeletal muscle

Cryostat sections (6 μm) were first incubated in the medium containing 0.1% manganese chloride, 0.1% hydrogen peroxide and 5.5 mM of diaminobenzidine tetrahydrochloride in 0.1 M sodium acetate pH 5.6 at 37°C for 60 min. The sections were washed in distilled water, incubated in 1% copper sulfate medium for 5 min, dehydrated in a graded ethanol series (70, 80, 90 and 100%) and cleared in xylene.

Quantitative RT-PCR

Total RNA was extracted from the cells using the RNeasy Mini Kit (Qiagen) and from mouse spinal cords and skeletal muscles using TRIzol (Invitrogen). The extracted RNA was then reverse-transcribed into first-strand cDNA using the SuperScript III First-Strand synthesis system (Invitrogen). RT-PCR was performed in a total volume of 25 μl that contained 12.5 μl of 2× QuantiTect SYBR Green PCR Master Mix and 0.3 μM of each primer (Sigma–Aldrich, MO, USA); the amplified products were detected with the iCycler system (Bio-rad Laboratories, Hercules, CA, USA). The reaction conditions were as follows: 95°C for 1 min, 40 cycles of 15 s at 94°C, 15 s at 59°C and 30 s at 72°C. The expression level of the internal control β2 microglobulin was simultaneously quantified. The following primers were used: 5′ ctgtgagaccaacagcctga 3′ and 5′ aatgcgagtggtcttccatc 3′ for the cell and mouse PPARγ, 5′ acagctccaagaccaggaaa 3′ and 5′ ctgaagtcgccatccttag 3′ for the mouse PGC1α, 5′ gtgtgagccaggatatagaaagac 3′ and 5′ aagccgaacatactgaactgc 3′ for the cell and mouse β2 microglobulin. The weight of the gene contained in each sample was equal to the log of the starting quantity, and the standardized expression level of each cell and mouse was equal to the weight ratio of each gene to that of β2 microglobulin.

Microarray analysis of the mouse spinal cord and skeletal muscle

Gene expression in the spinal cords and skeletal muscles of untreated and PG-treated AR-97Q mice was assessed using a SurePrint G3 Mouse GE 8 × 60K Microarray (Agilent Technologies, Santa Clara, CA, USA). For each group (untreated AR-97Q and PG-treated AR-97Q), we examined the male mice at 13 weeks of age. Most of the 13-week untreated AR-97Q mice were very weak and had experienced profound muscle atrophy. The RNA from the spinal cord and skeletal muscle was isolated from three mice of each group using TRIzol (Life Technologies Corporation, Carlsbad, CA, USA) according to the manufacturer's specifications. The RNA samples were purified using the PureLink™ RNA Mini Kit (Life Technologies Corporation). The cDNA